A model of Endothelin-1-mediated focal ischemia in the mouse forelimb motor cortex

By

R. Brian Roome

A thesis submitted to the School of Graduate
Studies in partial fulfilment of the requirements
for the degree of Master of Science (Medicine)

Faculty of Medicine (Neuroscience)
Memorial University of Newfoundland

October 2013

i

Abstract

Ischemic stroke is a debilitating medical event with the majority of sufferers experiencing long-term disability and motor impairments. While front line treatment such as anti-embolic medication and rehabilitation can improve the condition, many individuals remain significantly disabled. Experimental therapies involving genetic interventions hold potential for treatment of ischemic stroke, but many therapies go untested due to a lack of small cortical ischemic injury models in the mouse. Models of ischemic stroke should be small, reproducible and produce measurable behavioural deficits in order to see recovery after therapy. Additionally, the injury should avoid damage to neural precursor cells (NPCs) which are often targeted by genetic approaches to modify their survivability and plasticity post stroke. This highlights the demand for a small cortical ischemic injury model in the mouse, where transgenic technologies can be used to their full potential. Existing models of ischemic injury, such as middle cerebral artery occlusion (MCAO) produce large amounts of ischemic damage, but may prove more difficult to regenerate and/or eliminate behavioural deficits post-stroke. Endothelin-1 (ET-1), a potent vasoconstrictive peptide, was used to induce ischemia in the mouse cortex. ET-1 injected into the mouse cortex produced a small but significant infarct. To determine whether ET-1-induced infarcts could produce behavioural deficits, injections were targeted to the mouse forelimb motor cortex (FMC) and the amount of infarct encompassing the FMC was correlated with behavioural deficits. To analyze this, two-dimensional topological maps of cortical infarct depth were created and the deeper parts of injury correlated with behavioural deficits. Using standard behavioural tests adapted for use with mice, the mouse staircase test was shown to correlate with FMC infarct location and depth. The mouse cylinder test of forelimb asymmetry did not correlate with FMC infarct location and depth; despite this, a new analysis termed paw-dragging did correlate with FMC infarct location and depth. The results demonstrated that the FMC is functionally subdivided such that staircase deficits correlated with damage to the anterior FMC as opposed to the posterior FMC. As well, a small cortical infarct produced by ET-1

induced NPC proliferation and migration. At 14 days post-injection, there were significantly more neuroblasts in the subventricular zone (SVZ) and the corpus callosum ipsilateral to injury. As NPCs proliferate and migrate toward ET-1-induced cortical infarcts, there is potential for therapeutic intervention to improve regeneration of lost tissue. This study provides a foundation for manipulating NPCs and analyzing their integration into the peri-infarct cortex.

Acknowledgements

I would like to thank Dr. Jackie Vanderluit for her invaluable support in preparing me for a career in science, and giving me the opportunity to succeed.

I would like to thank Craig Malone, Kristine Day, Jieying Xiong and Mahmudul Hasan for their help and mentoring, as well as all the other members of the Vanderluit lab.

I would like to thank members of Dr. Dale Corbett's lab, including Matthew Jeffers, Kris Langdon, Shirley Granter-Button and Dr. Dale Corbett for their help and sharing their expertise in models of ischemic stroke.

I would like to thank my advisory committee, Dr. Karen Mearow and Dr. John McLean.

Lastly, I would like to thank my family and friends, and especially Marissa Lockyer, whose support helped me immensely in completing this thesis.

Abbreviations

ANOVA   Analysis of variance

APAF-1 - Apoptotic protease-activating factor-1

ATP - Adenosine tri-phosphate

Bcl-2   B-cell lymphoma 2

BrdU   5-bromodeoxyuridine

CBF   Cerebral blood flow

Cux1   Cut-like homeobox 1

d - Days

Dcx - Doublecortin

Dlx2   Distal-less 2

DNA – Deoxyribonucleic acid

ET-1 – Endothelin-1

ET-A/B   Endothelin-receptor subtype A/B

FMC   Forelimb motor cortex

GFAP   Glial fibrillary acidic protein

h   Hours

IHC - Immunohistochemistry

MCAO   Middle cerebral artery occlusion

Mcl-1   Myeloid-cell Leukemia 1

NeuN   Neuronal nuclei

NPC   Neural precursor cell

NSC   Neural stem cell

1x PBS   Phosphate buffered saline

PFA - Paraformaldehyde

PSA-NCAM   Poly-sialated neural cell adhesion molecule

RMS   Rostral migratory stream

SGZ   Subgranular zone

SVZ – Subventricular zone

TAT – Transactivator of transcription

t-PA – Tissue-plasminogen activator

Tuj1   βIII-Tubulin

List of Figures

List of Tables

Chapter 1: Introduction

1.1 Adult neurogenesis and stem cells in the adult brain

1.1.1   Stem cells in the adult CNS

The adult brain is capable of regenerating cells throughout life. The prior consensus, that neurons were not generated after birth, was questioned repeatedly during the 1960s and ultimately upended in the 1990s. The candidate cell type which can generate neurons after birth is the neural stem cell (NSC). Neural stem cells are self-renewing cells which have the ability to differentiate into multiple brain-specific cell subtypes: neurons, astrocytes and oligodendrocytes (Reynolds & Weiss, 1992). These cells continuously supply parts of the brain with new neurons and glial cells throughout life. In the 1960s, work with ^{3}H-thymidine (Altman, 1962) autoradiography showed signal-retaining cells within the dentate gyrus of the adult rat hippocampus which declined in number with age (Altman & Das, 1965). Cells within the adult rat subventricular zone (SVZ) lining the lateral ventricles were also observed to be label-retaining and declined in number with age (Altman, 1963; Altman & Das, 1966). As well, labeled cells decreased in number rapidly after the ^{3}H-thymidine injection suggesting a fate of death or migration. Evidence for a path of migratory cells toward the olfactory bulb (rostral migratory stream or RMS) was found using autoradiography (Altman & Das, 1969). While Altman's studies correctly identified mitotic characteristics of the SVZ, the type of cells within the SVZ was not yet determined.

Neural stem cells were characterized as SVZ-derived cells which could proliferate in the presence of EGF as well as differentiate and express markers of neurons and astrocytes such as enolase-2 and glial fibrillary acidic protein (GFAP), respectively (Reynolds & Weiss, 1992). The proliferative cells of the SVZ were demonstrated to be stem cells by the ability to self-renew indefinitely in the presence of EGF, and the ability to remain multipotent (Reynolds & Weiss, 1996). The proliferative population could be replenished after ablation and was considered to be primarily neural progenitor cells

1

(NPCs). These cells are fate-restricted progeny of stem cells with a finite capacity to self-renew. A small quiescent population of SVZ cells were found to comprise the stem cell population (Morshead et al., 1994). Together the stem cell population and the progenitor population are termed "neural precursor cells" (NPC). The current study will investigate neurogenesis primarily in the SVZ.

1.1.2 The SVZ niche

The NPCs within the SVZ are supported by multiple cell types which maintain their homeostasis. This heterogeneous population of cell types, or "niche" is maintained into adulthood and is responsible for the self-renewal of NSCs and maturation of their progeny. NPCs are supported by a unique vasculature, by niche astrocytes and the ventricular ependyma. Through regulation of proliferation, growth and stem cell identity, the SVZ persists throughout one's lifespan.

The SVZ is located between the ciliated ependymal cell layer facing the ventricle and the striatal parenchyma. Within the niche, there are four major cell-types (Fig 1.1). Type B cells are the resident NSCs (less than 1% of cells, Morshead et al., 1994) which divide slowly and give rise to Type C cells. Using cumulative doses of 5-bromodeoxyuridine (BrdU, a thymidine analog), a rapidly dividing progenitor population the type C cell population was described (Morshead & van der Kooy, 1992). Type C cells, also known as the transit-amplifying cells, give rise to Type A cells. Type A cells are neuroblasts which migrate along the RMS to the olfactory bulb, where they terminally differentiate into neurons (Fig. 1.1). Glial Fibrillary Acid Protein (GFAP)+ cells within the SVZ were found to be the residing NSC in the SVZ. These GFAP+ cells can form neurospheres *in vitro* (Doetsch et al., 1999a; Morshead et al., 2003) and can repopulate the lineage of C and A cells (Doetsch et al., 1999b). Type E cells are the ependymal cells that line the ventricular wall of the SVZ (Doetsch et al., 1997) and have low proliferative ability and no multipotency (Chiasson et al., 1999) under normal circumstances. The cell types described above are characterized by specific immunohistochemical markers, electron-micrograph markers and distinct cell cycle lengths. Type B cells express GFAP,

Figure 1.1: Morphology and lineage of the SVZ Niche. Neural stem cells (type B) divide slowly and give rise to transit-amplifying cells (type C), which divide rapidly. Transit-amplifying cells divide and differentiate into neuroblasts (type A), which gain the ability to migrate in chains. Ependymal cells (type E) face the lateral ventricles, form tight junctions with each other, and do not belong to the neural stem cell lineage (adapted from Doetsch et al., 1999a).

SVZ Astrocyte   Immature Precursor   Migrating Neuroblast
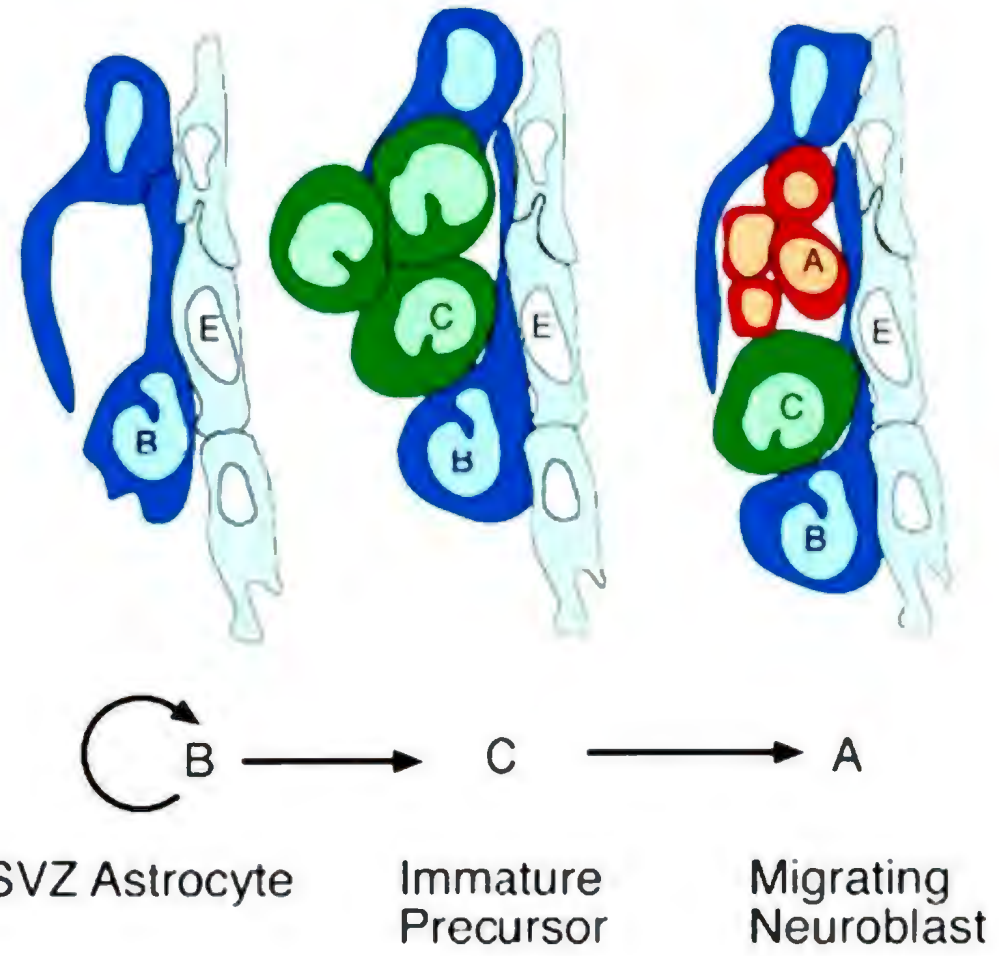
Figure 1.1

Sox21 and Nestin, but not distal-less 2 (Dlx2). The C cells (transit-amplifying cells) express (Dlx2) but not polysialated neural cell adhesion molecule (PSA-NCAM) like their neuroblast progeny (Table 1.1, modified from Okano et al., 2007). Neuroblasts express PSA-NCAM and Doublecortin (Dcx) and migrate toward the olfactory bulb to become mature neurons, which express NeuN. Electron micrographs reveal other morphological differences: neuroblasts have small elongated nuclei and a dark cytoplasm, while type B and C cells have large nuclei and a bright cytoplasm. Cell cycle length can also distinguish between GFAP+ type B cells and Dlx2+ type C cells in that their cell cycle times are 28 days (Craig et al., 1994) and 12.7 hours respectively (Morshead & van der Kooy, 1992). Targeting and experimenting with NPCs in the SVZ is possible using these precise markers.

The SVZ niche is regulated by a host of growth-promoting factors. Within the cerebrospinal fluid, Insulin-like growth factor-II (IGF-II) regulates growth by binding to receptors on NSC primary cilia projecting into the lateral ventricle (Lehtinen et al., 2011).

Table 1.1: Markers of the SVZ lineage.

	Neural Stem Cell	Transit-amplifying Cell	Neuroblasts	Immature Neuron	Neuron
GFAP	+				
Sox21	+	+	+		
Nestin	+	+	+		
Dlx2		+	+		
PSA-NCAM			+		
Doublecortin			+		
BetaIII-Tubulin				+	
NeuN					+
Electron-micrograph details	Large Nucleus Bright Cytoplasm	Large Nucleus Bright Cytoplasm	Small Nucleus Dark Cytoplasm		
Cell Cycle Time	28 days	12.7 hours	Post-mitotic	Post-mitotic	Post-mitotic

EGF and FGF2 both increase proliferation within the intact brain (Craig et al., 1996; Kuhn et al., 1997) and have also been shown to be crucial factors for maintaining adult NPCs in a proliferating undifferentiated state *in vitro* (Gritti et al., 1995; Reynolds & Weiss, 1992). Notch pathway activation is required for self-renewal of NSCs (Imayoshi et al., 2010). A variety of other ligands regulate proliferation in the SVZ, including Sonic Hedgehog (Palma et al., 2005), Wnt ligands (Adachi et al., 2007) and vascular endothelial growth factor (Jin et al., 2002). The proliferation in the SVZ directly contributes to the maturation of olfactory bulb interneurons, as newborn neuroblasts migrate toward the olfactory bulb.

1.1.3   SVZ progeny repopulate the olfactory bulb interneurons via the RMS

New neurons, derived from SVZ neuroblasts, develop within the olfactory bulb. In particular these neurons are found within the granule and periglomerular layers. Between the SVZ and the olfactory bulb, neuroblasts form a long moving chain – the RMS. In 1994, the RMS was discovered to consist of SVZ derived neuroblasts (Lois & Alvarez-Buylla, 1994). This led to a series of mechanistic discoveries about how NPCs become olfactory bulb neurons. Using immunohistochemical analysis, neuroblasts were observed to migrate in a chain-like procession sheathed in a GFAP+ astrocyte cage (Lois et al., 1996). Chains of migrating neuroblasts are found throughout the SVZ and converge at the RMS. To demonstrate this, NPCs expressing LacZ under the neuron-specific enolase promoter were grafted into the caudal SVZ of wild-type animals. This resulted in granule and periglomerular labeling within the olfactory bulb thirty days after the graft (Doetsch & Alvarez-Buylla, 1996). While many factors involved in proliferation and migration have been elucidated, little is known about the regulation of survival of NPCs. The option to live or die by apoptosis is integrated through the Bcl-2 family of proteins. Understanding which factors mediate a NPC's fate to live or die could ultimately have therapeutic benefits for neurodegenerative disease.

1.2 - Ischemic stroke

Stroke results from an interruption of blood flow to the brain (ischemic) or busting of blood vessels within or around the brain (hemorrhagic) causing cell death. Strokes are commonly ischemic (87%), and most often caused by embolism. A minority of strokes are hemorrhagic (13%), in the case where a blood vessel is broken by trauma, hypertension or the result of a ruptured aneurysm (Rosamond et al., 2008). The majority of ischemic strokes are serious if not fatal: 18% of patients die post stroke. The remaining 82% of stroke patients survive. While 42% of patients return to their life with little to no impairment, 40% are admitted to long-term care. Overall statistics suggest that 1 in 18 deaths are stroke-related (Roger et al., 2011). Age is one of the most pertinent predictors of stroke - risk of stroke doubles every ten years past the age of 55 (Sacco et al., 1997). The Canadian population is aging rapidly: population growth for those 65 and older has been 14.1% contrasted with the overall Canadian population growth rate of 5.9% between 2006 and 2011 (Statistics Canada, 2012). As a result, the burden of stroke on the health care system is becoming a more pressing issue

The current front line treatment for acute ischemic stroke is tissue-plasminogen activator (t-PA). T-PA is effective within a 4.5 hour window after ischemic stroke, and serves to break down fibrin clots and mitigate stroke-related symptoms by activating serum plasmin. Efficacy is greatly reduced when given 3 hours post stroke and when given after 4.5 hours there is no significant effect. Despite this being the front line treatment for ischemic stroke, reperfusion occurs only 46% of the time (Vivien et al, 2011). Additionally, there is a 6.4% chance of intracerebral hemorrhage with a 50% survival rate if this occurs. While t-PA is a valuable front line treatment, many patients do not arrive in a hospital in time for t-PA to be effective. As well, only 32% of patients given t-PA have an improved clinical outcome. The necessity for developing therapies which are effective outside the 4.5 h window of t-PA is paramount. Apart from acute pharmacological therapy with t-PA, behavioural rehabilitation is able to restore some lost functionality. As behavioural therapy does not result in a complete recovery, new investigations involve repairing the site of injury. Understanding the cellular pathophysiology of ischemic stroke is critical in developing therapies preventing cell

7

death or regenerating lost cells.

1.2.1 - Pathophysiology of ischemic stroke

The pathophysiology of ischemic stroke consists primarily of neuronal death, when cerebral blood flow (CBF) drops below a threshold. Necrotic cell death occurs within the core of the ischemic region as early as 3h post-ischemia after the permanent occlusion of the middle cerebral artery in the rat (Lipton, 1999). Neurons surrounding this region are vulnerable to toxic metabolites released from dying neurons — this is the penumbra, characterized by a prolonged, mostly apoptotic, mode of cell death. The extent to which perfusion is reduced, as well as the time during which the artery is occluded determine the extent of cell death.

Damage begins after arterial occlusion, resulting in a core of necrotic tissue caused by loss of perfusion and inflammation. This damage is first seen at about 3h post-occlusion in rats, which corresponds to the effective time course of t-PA in humans (indicated for less than 3h after onset of symptoms). The core of the ischemic region is "infarcted", a term describing dead and damaged tissue. The infarct is characterized histologically by pale cresyl violet staining, which is associated with necrosis and vacuolization of neurons and glia (Lipton, 1999), as well as energy failure (ATP depletion), less than 15-20% normal CBF and irreversible tissue damage (Lipton, 1999; Moskowitz et al., 2010). Surrounding the core is the penumbra, a partially ischemic region which is vulnerable to toxic metabolites and inflammation within the core (Fig 1.2). Cells within the penumbra maintain ATP homeostasis and membrane polarity (Astrup et al., 1981). The penumbra receives between 15% to 40% of normal CBF which causes action potentials to cease (Astrup et al., 1977). The duration of ischemia without reperfusion affects how and when neurons in the penumbra die. After permanent artery occlusion, the infarcted core is visible within 3-12h. The infarct then spreads to encompass most of the penumbra after 6-24h from the time of artery occlusion, and expands through the remaining penumbra over 24-72h (up to 30% of the infarct volume). By limiting the time of artery occlusion, cell death can be prevented or delayed.

Figure 1.2: Diagram of ischemic stroke – core vs penumbra. (A) The necrotic core forms within hours, while the penumbra is viable but has no neural activity. (B) Between 24-72h post-ischemia, the infarct has encompassed most of the penumbra. Light gray denotes viable tissue with less than 40% normal CBF. Dark gray denotes dead (infarcted) tissue.

A

B
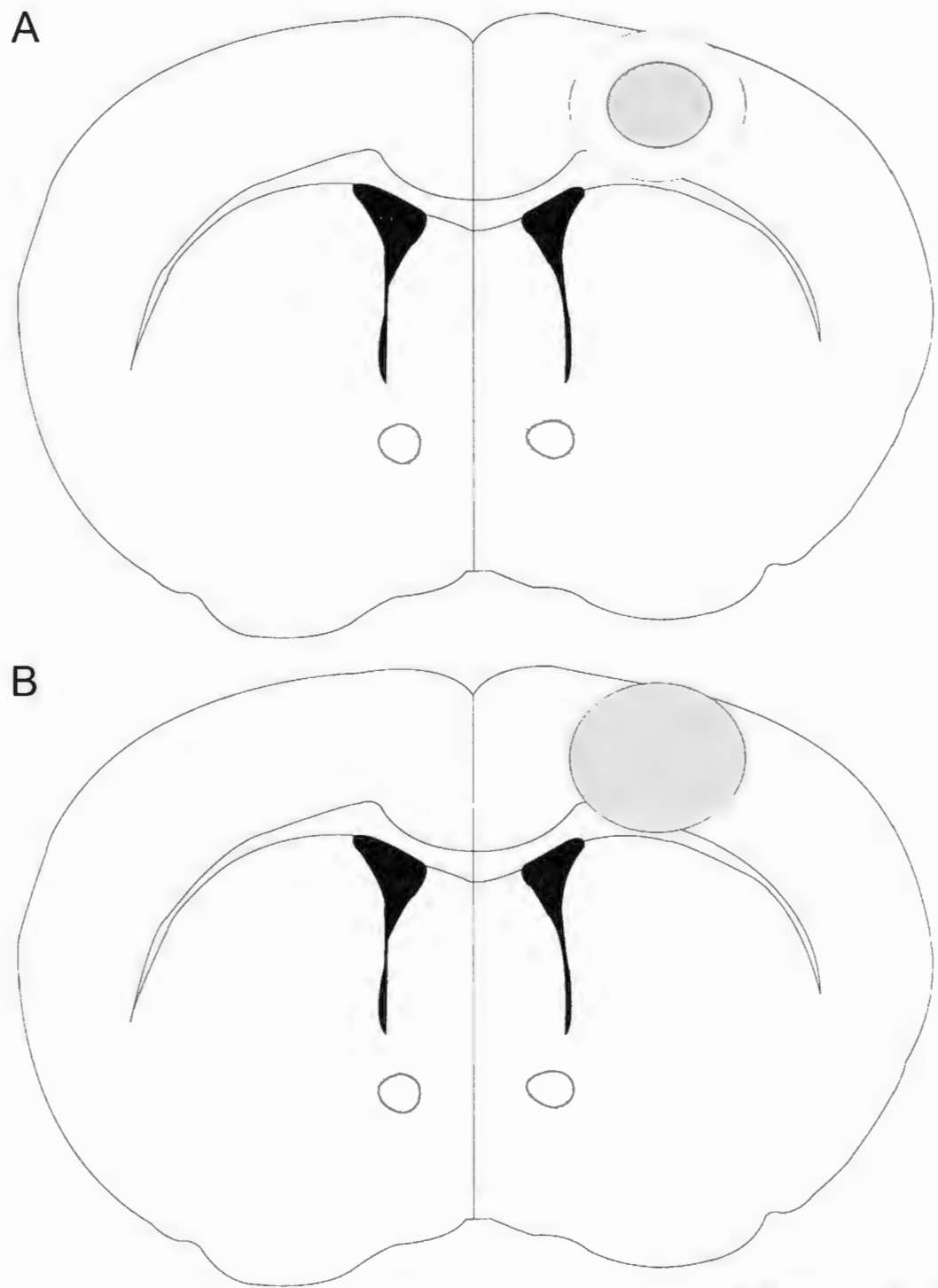
Figure 1.2

T-PA is useful in preventing cell death because it limits the amount of time that arteries are occluded. After 10-20 minutes of artery occlusion a minority of neurons within the core are necrotic. After an hour of artery occlusion, the infarct encompasses the core and after a 2-3h artery occlusion the infarct will expand into the penumbra (though it expands more slowly than permanent ischemia, Lipton, 1999). Viability of the penumbra therefore, in the absence of treatment, is tightly linked to the amount of time before normal blood flow is restored. The penumbra is a therapeutically useful region because it is possible to prevent cells within it from dying. Timely administration of t-PA is an important factor in preventing penumbral cell death.

The type of cell death in ischemic stroke varies temporally. Necrosis is the more predominant form of cell death in older animals (Yuan, 2009). Using common carotid artery occlusion, it was shown that older rats develop more necrotic death within the hippocampus than younger rats, which had more apoptotic cell death (Liu et al., 2004). Though the levels of cerebral blood flow were not examined in this study, cell death peaked at 24-48h post-ischemia, suggesting the region of interest is the penumbra. The penumbra has sufficient perfusion to keep cells alive (Moskowitz et al., 2010); however, toxic extracellular signals such as glutamate released from the necrotic core can induce additional neurons to undergo necrotic, apoptotic and excitotoxic cell death. Apoptotic cell death is associated with mild lesions and brief ischemic insults (Moskowitz et al., 2010) and occurs predominantly in the penumbra (Dirnagl et al., 1999; Yuan, 2009). Most apoptotic cell death occurs between 24-72h post-ischemia, but levels can be significantly maintained over a week afterward (Dirnagl et al., 1999, Liu et al., 2004). Due to the viability of the penumbra after stroke, there is therapeutic interest in using anti-apoptotic proteins to prevent apoptosis during this time.

1.2.2   Apoptotic cell death

Apoptosis is a form of energy-dependent cell death. The B cell lymphoma-2 (Bcl-2) and caspase families of proteins are major families of proteins executing apoptosis. Apoptosis proceeds by activating pro-apoptotic Bcl-2 family proteins in response to

cellular stress – this triggers caspase activation and cleavage of multiple substrates required for cell survival. Within the Bcl-2 family, proteins share conserved Bcl-2 homology (BH) domains. This family of proteins consists of two classes: the anti-apoptotic proteins and the pro-apoptotic proteins. Of the pro-apoptotic proteins, two subclasses exist: the effector proteins which have BH domains 1-3, and the BH3-only proteins. The anti-apoptotic proteins are identified by BH domains 1-4 (Chipuk et al., 2010; Ulukaya et al., 2011).

The role of the pro-apoptotic effector proteins, Bak and Bax, are to induce apoptosis by opening a large channel in the outer mitochondrial membrane. Bak and Bax form oligomers while embedded in the outer mitochondrial membrane, opening channels which allow proteins to exit the mitochondrial intermembrane space (Youle & Strasser, 2008). The BH3-only proteins recruit pro-apoptotic effector proteins and facilitate oligomerization. They act as mediators for cellular stress responses, and relay these signals to the pro-apoptotic effectors. Anti-apoptotic proteins act to sequester BH3-only proteins from promoting apoptosis (Chipuk et al., 2010). These proteins (with the exception of A1) have a C-terminal transmembrane domain, anchoring them to the outer-mitochondrial membrane, where they can associate with and inhibit Bax/Bak or the BH3-only proteins (Youle & Strasser, 2008).

Apoptosis is ultimately triggered by the Bcl-2 family of proteins, but a complex signalling cascade links the Bcl-2 family to destruction of the cell. The intrinsic and extrinsic apoptotic pathways end with activation of caspases – cysteine proteases which cleave a diverse range of substrate proteins after an aspartic acid residue (Ulukaya et al., 2011). The intrinsic pathway of apoptosis is a cellular signalling pathway downstream from Bax/Bak's initiation of apoptosis (Fig 1.3). After Bak/Bax homo-oligomers form pores within the outer mitochondrial membrane, the signaling cascade begins. Cytochrome C release induces formation of the apoptosome, a protein complex consisting of seven cytochrome C/Apoptotic protease-activating factor-1 (APAF-1) dimers. APAF-1 activates caspase-9, which then activates caspases-3 and/or -7, which cleave a wide range of substrates resulting in cell death (Taylor et al., 2008; Youle & Strasser, 2008). Apoptosis can be detected by analyzing the downstream effects of

Figure 1.3: The intrinsic pathway of apoptosis. Anti-apoptotic proteins bind and inhibit BH3-only and pro-apoptotic proteins from initiating apoptosis. Prior to apoptosis, Bak/Bax oligomerize and insert into the outer-mitochondrial membrane. Pores formed by Bak/Bax allow cytochrome C release from the mitochondria, apoptosome formation and widespread caspase activation. Adapted from Youle & Strasser (2008).

Intrinsic pathway

Growth-factor deprivation, stress, UV, viruses

Inactive BH3-only → Active BH3-only

⊣ BCL-2

⊣ BAX/BAK

Cytochrome *c* release, mitochondrial fragmentation

Cytochrome *c* — APAF1

APAF1 assembly into apoptosome

Caspase-3

Apoptosis

Figure 1.3

14
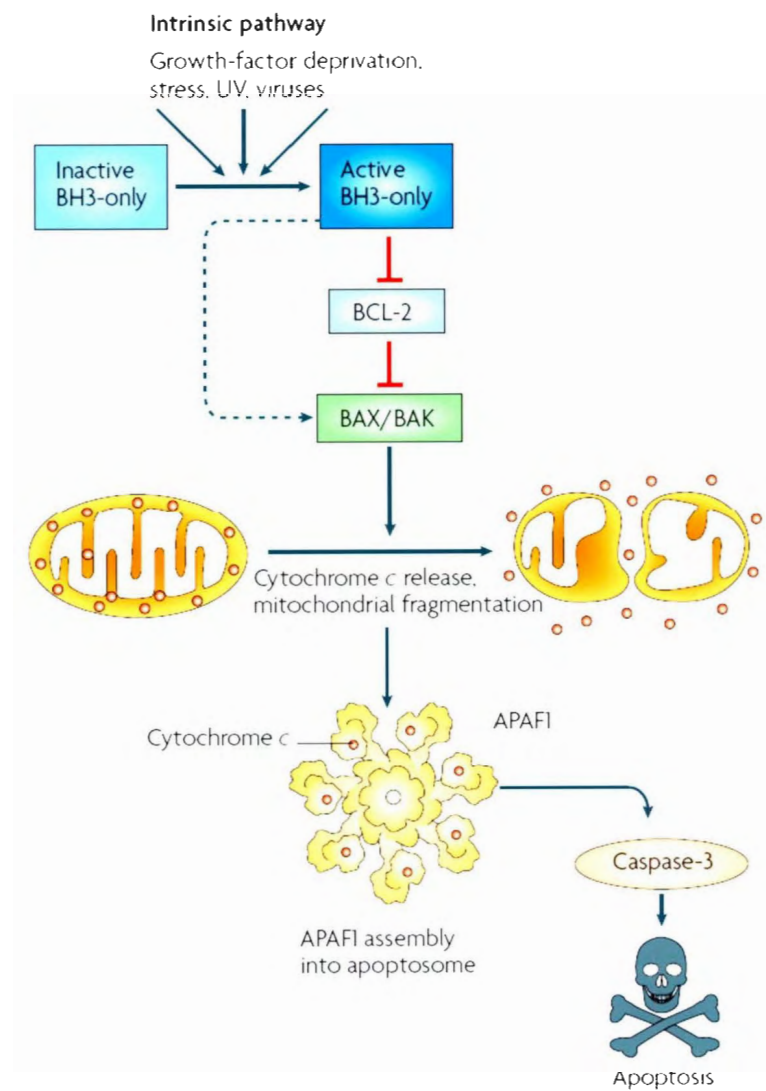
multiple substrate cleavage. By cleaving cytoskeletal and cytoskeletal-associated proteins, the cell rounds and, withdraws its processes. This produces membrane blebbing which results in cell fragments called apoptotic bodies. The nucleus is observed to condense and subsequently fragment. DNA is cleaved between histones, producing "laddering" of DNA on a gel — fragments of lengths in multiples of 200bp. Apoptotic bodies are engulfed by neighbouring cells and macrophages. This is triggered by presentation of phosphatidylserine on the outer layer of the plasma membrane (normally it is found only on the inner layer). Inflammation is associated with necrotic cell death when cytosolic proteins diffuse out of a dying cell. Since apoptotic bodies are rapidly engulfed by macrophages, inflammation is avoided (Taylor et al., 2008).

1.2.3   Preventing apoptosis after ischemic stroke

Treatments are in development to prevent apoptosis in the penumbra and some consist of delivering anti-apoptotic Bcl-2 family proteins to the injury site. Transfecting SVZ NPCs with Bcl-2 before middle cerebral artery occlusion (MCAO) results in increased numbers of Dcx+ neuroblasts and Tuj1+ immature neurons in the ischemic striatum, and reduced apoptotic active caspase-3+ immature neurons (Zhang et al., 2006). A fusion protein consisting of a fragment of Transactivator-of-transcription (TAT) protein from the Human Immunodeficiency Virus and Bcl-xL (TAT-Bcl-xL), recovery can be attained in rodent stroke models (Doeppner et al., 2009; Kilic et al., 2002). A protein transduction domain of TAT is used, allowing the peptide to penetrate cell membranes. The intravenous application of TAT-Bcl-xL was shown to reduce infarct size as well as apoptosis within the damaged striatum of mice following middle cerebral artery occlusion. Treatment improved motor function lost after MCAO as assessed by rota-rod and elevated beam tests (Doeppner et al., 2009). After TAT-Bcl-xL treatment, increased survival of striatal neurons (Kilic et al., 2002) and increased survival of Dcx+ neuroblasts (Doeppner et al., 2009) was observed, suggesting that functional recovery occurred.

NPC proliferation occurs in the SVZ after occlusion of the middle cerebral artery,

which produces an ischemic injury in rodents (Jin et al., 2001, Gordon et al., 2007). As well, after MCAO, Dcx+ neuroblasts migrate from the SVZ to the peri-infarct cortex and differentiate into neurons and glia (Gordon et al., 2007; Zhang et al., 2007). While treatment with TAT-Bcl-xL increases survival of migrating Dcx+ neuroblasts after MCAO (Doeppner et al., 2009) it has not resulted in increased gliogenesis, as marked by NG2 immunohistochemistry. A treatment which preferentially increases neurogenesis should stand to improve functional recovery. While protecting neurons in the penumbra is an exciting way to prevent long term disability, the latency to detect and treat stroke prevents treatment from being given in a timely manner. Harnessing the endogenous neurogenic response to CNS injury and using treatments to improve this response can expand the time window in which stroke can be treated.

1.2.4 - Mcl-1

Myeloid cell leukemia 1 (Mcl-1) is an anti-apoptotic member of the Bcl-2 family of proteins, classified based on its high sequence homology to Bcl-2 (Kozopas et al. 1993). It has been shown to be a critical survival factor for embryonic NPCs (Arbour et al., 2008). In addition to using proteins of the Bcl-2 family to prevent penumbral apoptosis, Mcl-1 could be used therapeutically to protect NPCs during the endogenous neurogenic response to injury (see section 1.3).

Mcl-1 mRNA is enriched within developing NPCs and immature neurons in the developing telencephalon (Arbour et al., 2008). Since Mcl-1 germline knockout results in early embryonic lethality (Rinkenberger et al, 2000), an Mcl-1 conditional knockout was made using Mcl-1$^{(f/f)}$ mice crossed with transgenic Nestin Cre mice. Nestin, an intermediate filament, is expressed within the NPC population. When Cre-mediated deletion of Mcl-1 occurred within embryonic NPCs, 15-25% of Nestin+ cells died via apoptosis. Furthermore, significant numbers of Dcx+ neuroblasts and Tuj1+ immature neurons initiated apoptosis when Mcl-1 was knocked out (Arbour et al., 2008). Mcl-1 plays the same role in adult NPCs. Mcl-1 is required for survival of NPCs in the intact adult brain of Mcl-1$^{(f/f)}$ mice, verified by electroporating the adult SVZ with a Nestin Cre

16

plasmid and assessing levels of apoptosis. Mcl-1 gain-of-function in adult-derived NPC culture also reduced apoptosis (Malone et al., 2012). These results highlight the role of Mcl-1 as a survival factor in neural stem and progenitor cell populations within the developing and adult brain. In comparison to Mcl-1, other anti-apoptotic Bcl-2 family members such as Bcl-2 (Michaelidis et al., 1996) and Bcl-xL (Savitt et al., 2005) are required for survival of post-mitotic neurons. Specifically, Bcl-2 knockout mice have been shown to have increased apoptosis of sensory and sympathetic neurons, while Bcl-xL conditional knockouts using a Tyrosine Hydroxylase Cre transgenic mouse result in 30% fewer catecholaminergic cells in the substantia nigra. Together, these results show that Mcl-1 has an endogenous role in promoting survival in NPCs. After CNS injury, a neurogenic response occurs whereby NPCs from the SVZ migrate and differentiate in the peri-infarct tissue, though most NPCs die when reaching the site of injury (Arvidsson et al, 2002). Promoting survival by transfecting NPCs with Mcl-1 could improve their viability in the ischemic penumbra and allow newborn neurons to integrate into local circuits.

1.3   Stroke induced neurogenesis

A variety of insults to the telencephalon can induce NPCs within the SVZ and SGZ to proliferate. Moreover cells within the SVZ have been shown to migrate toward the site of injury and differentiate into mature neurons and glia. Exploiting the injury response in the CNS is an attractive strategy to repair the CNS after damage.

1.3.1   Neural precursor cells proliferate after CNS injury

NPCs in the CNS proliferate in response to injury. This was demonstrated after cortical aspiration lesions in rats, where an increase in PSA-NCAM+ cells in the ipsilateral SVZ was observed post-aspiration (Szele & Chesselet, 1996). Since then, a host of studies have demonstrated an increase in SVZ proliferation under a variety of conditions (Gordon et al., 2007; Jin et al., 2001; Kreuzberg et al., 2010; Liu et al, 1998;

Tonchev et al. 2003; Wang et al., 2007b; Zhang et al, 2001). Quinolinic acid (an NMDA agonist) used in a model of glutamate excitotoxicity induces SVZ proliferation in striatal lesions up to one day post lesion in rats (Gordon et al., 2007). MCAO which is widely used in rodents also induces NPC proliferation. Proliferation after MCAO increased SGZ & SVZ proliferation in gerbils (Liu et al., 1998) and rats (Jin et al., 2001, Zhang et al., 2001). The response in the rat revealed a doubling of the number of Dcx+ neuroblasts in the ipsilateral SVZ 14d after MCAO (Zhang et al., 2004). A proliferative response was also observed in the macaque after global ischemia (Tonchev et al., 2003, (Tonchev et al, 2005). Similarly, an ET-1 mediated cortical ischemic injury produced an increase in ipsilateral SVZ proliferation in the mouse (Wang et al., 2007b). These results show that NPCs respond to CNS damage by proliferating, and that this response is conserved in several mammalian species. This effect is noteworthy in the injured brain in that NPCs can migrate away from the SVZ, move into damaged tissue and differentiate into cells of the neural lineage.

1.3.2   Neural precursor cells migrate away from the SVZ and differentiate after CNS injury

 In addition to proliferation, NPCs have been shown to migrate toward damaged CNS tissue. Early studies produced evidence for neurogenesis following ischemia, but did not demonstrate the origin of the newborn neurons. Neurogenesis was demonstrated by BrdU administration post thrombotic-stroke in rats, as cells co-labeled for BrdU+ and NeuN+ (a mature neuronal marker) were observed in the lesioned cortex 100 days post-photothrombolytic ischemia (Gu et al., 2000) and post-MCAO (Jiang et al, 2001). Soon after, studies using MCAO in the rat demonstrated BrdU+/NeuN+ cells in the injured striatum as well (Arvidsson et al., 2002, Parent et al, 2002). Moreover, adjacent to the SVZ, chains of Dcx+/BrdU+ neuroblasts extended into the striatum toward the damaged tissue, suggesting that the newborn neurons were of SVZ origin (Arvidsson et al., 2002). The peak number of migrating neuroblasts occurs 7-14 days post-MCAO (Zhang et al., 2004), suggesting that this neurogenic response occurs rapidly, soon after ischemia. The

neuroblasts which migrated toward the cortex post-MCAO were found to be between 1.5-2.5% of the BrdU+ cells within the peri-infarct tissue with the majority of BrdU+ cells found to be microglia (Kreuzberg et al., 2010). These neuroblasts were traced using transgenic mice expressing EGFP under the 5HT3A promoter (5-HT receptor 3A, expressed by a subset of SVZ neuroblasts and GABAergic interneurons) to mark neuroblasts. BrdU was used to identify newborn EGFP+ neuroblasts. Using the 5HT3A-EGFP mouse, MCAO resulted in EGFP+/NeuN+/BrdU+ neurons in the ischemic cortex, demonstrating that cortical/striatal neurogenesis post-ischemia was SVZ-derived. The source of migrating NPCs was revealed using retroviral vectors to insert the GFP gene into NPCs in the SVZ (Goings et al., 2004, Gordon et al., 2007). By labeling SVZ NPCs with a fluorescent marker such as GFP, the source of GFP+ cells which have migrated can be said to have originated from the SVZ. Recently, studies have demonstrated some causes of neuroblast migration: factors released during angiogenesis, notably stromal-derived factor-1 (SDF-1) and Angiopoietin-1, attract neuroblasts which express their cognate receptors (Ohab et al, 2006). These findings demonstrate that SVZ-derived NPCs are the cells migrating and differentiating in the peri-infarct tissue, that NPCs are rapidly mobilized for a short period of time, and that migration is mediated by chemotaxic factors released during peri-infarct angiogenesis.

Exploiting the migratory response for therapy was shown to be time-sensitive, as neuroblasts differentiate into glia more often at later time points. The fate of SVZ progeny can be traced by injecting retroviruses carrying the GFP gene into the SVZ. Neuroblasts can then be located after migrating away from the SVZ if they are GFP+. In a model of quinolinic acid-induced cell death in the striatum, SVZ cells were observed to migrate toward the injury. At five days post-SVZ infection with retrovirus, the location of GFP+ cells was analyzed (Gordon et al., 2007). When the SVZ was infected 2 days prior to injury or on the day of injury, the majority of migrating cells expressed GFP and Dcx (indicating neuroblasts migrating from the SVZ). In contrast, an infection 2 days post-lesion resulted in 99% of GFP+ cells being Dcx- and having a glial morphology (Gordon et al., 2007). This demonstrates that neurons are produced in a time-sensitive manner after injury and therapies delivered immediately after ischemia may have the greatest

impact on neurogenesis.

1.3.3 The majority of neural precursor cells die when migrating toward a CNS injury

Despite the ability of NPCs to migrate toward the injured cortex and striatum, the fraction of cells which survive to maturity is low. Following MCAO in rats, Dex+ cells were monitored in the ischemic striatum. There were approximately 4000 Dex+/BrdU+ cells in the ischemic striatum 2 weeks post-MCAO, whereas, at 6 weeks post-MCAO, the number of NeuN+/BrdU+ neurons was approximately 800. Thus, in the ischemic striatum, 80% of migrating neuroblasts do not become mature neurons (Arvidsson et al., 2002). These results highlight a challenge toward using NPCs therapeutically to improve post-stroke recovery: how to prevent the death of neuroblasts and newborn neurons. Of the surviving mature neurons, half of the NeuN+/BrdU+ cells expressed DARPP32, a marker for mature striatal medium spiny neurons. This demonstrates that SVZ NPCs have the ability to differentiate into area-specific subtypes - therefore urging NPCs to differentiate into a desired subtype may be an avoidable hurdle to therapy. However, since the vast majority of cells do not become mature neurons, therapy with pro-survival proteins could dramatically boost the number of mature neurons post-stroke.

Inflammation has been linked to high levels of migrating neuroblast apoptosis post-injury. Mice depleted of CD4+ T-lymphocytes (lymphocytes involved in inflammatory cytokine release and macrophage activation) were studied after MCAO. Apoptosis was reduced by 50% in neuroblasts migrating toward the infarct boundary (Saino et al., 2010). This reveals that the environment near the site of injury promotes neuroblast death and further reveals the need for anti-apoptotic therapies for post-stroke NPC survival.

Treatments involving Bcl-2 overexpression in NPCs have decreased apoptosis in the hippocampus post-MCAO (Sasaki et al., 2006). Overexpression of Bcl-2 family members may, therefore, reduce apoptosis in SVZ-derived NPCs. We have previously shown that Mcl-1 is a critical survival factor for adult NPCs in the SVZ (Malone et al., 2012). Type B, C and A cells within the SVZ express Mcl-1. When NPCs were

transfected with Cre in an Mcl-1 floxed mouse, the rate of NPC apoptosis was increased two-fold. As well, when cultured NPC's overexpressed Mcl-1, apoptosis decreased three-fold. These data suggest that Mcl-1 is a crucial survival factor for NPC's, and may be useful in increasing their survivability. Therefore, overexpressing Mcl-1 in the SVZ after cortical injury has the potential for increased regeneration of neurons, as migrating neuroblasts and immature neurons are otherwise vulnerable to apoptosis.

1.3.4   Gene delivery to the SVZ has therapeutic potential

Regeneration of cortical tissue can be studied by observing neurogenesis and gliogenesis in the peri-infarct cortex or striatum. Since many neuroblasts leaving the SVZ die before they become mature neurons, therapies that improve their survival are warranted. One method that can be used is gene therapy: introducing pro-survival genes into NPC's before or during their migration toward the peri-infarct cortex. Improving NPC survival via gene therapy is an attractive method to regenerate more neurons post-ischemia. In order to introduce genes into NPC's, the lateral ventricle wall can be targeted. These NPC's may integrate successfully into existing circuits, translating into measurable behavioural recovery on forelimb motor control tasks, which is the ultimate goal of regenerative therapy.

Gene delivery targeting type B cells can be performed via *in vivo* electroporation. This process involves injecting plasmid DNA into the lateral ventricle and administering an electric pulse across the head (Fig. 1.4). While 95% of cells transfected are ependymal cells (Barnabe-Heider et al., 2008), a minority of transfected cells are type B cells which make contacts with the ventricle. After passing genes on to type C and type A cell progeny, the efficacy of exogenous genes in improving type A cell (neuroblast) viability can be assessed. Previously our laboratory (the Vanderluit laboratory) has used adult electroporation to knock out Mcl-1 in the adult NPC population. Using plasmid DNA containing Cre expressed under the Nestin promoter, the plasmid was electroporated into the SVZ in an Mcl-1$^{fl/fl}$ mouse where Cre expression was observed in NPC's (Malone et al., 2012). As genes expressed under the Nestin promoter will only be expressed in the

NPCs, and not the ependymal cells lining the ventricle, this demonstrates that adult electroporation can deliver genes to NPCs. Using this technique to trace neuroblasts migrating from the SVZ toward the injury site would demonstrate that neuroblast gene therapy is possible post CNS injury. Furthermore, our laboratory has shown that transfection of Mcl-1 into NPCs *in vitro* increases their survival 3-fold (Malone et al., 2012). This work sets the precedent that Mcl-1 overexpression in NPCs can increase survival and that it can be reliably introduced into type B cells *in vivo*. Using an ischemic cortical injury model to induce NPC proliferation and migration, the effects of Mcl-1 on NPC survival after migrating into infarcted tissue can be assessed. However, to assess Mcl-1's effect on functional stroke recovery, a cortical injury model with relevant behavioural assessments must first be selected.

1.4   Appropriate models of CNS injury & repair in mice

1.4.1 - Models of focal cerebral ischemia

In selecting a model of focal ischemic injury, three criteria should be met: (1), that a small reproducible ischemic injury can be produced; (2), that the injury correlates with relevant reproducible behavioural deficits; and (3), that the neural precursor population is not damaged during the injury, as they are required to regenerate injured neural tissue. While ischemic injury models available today have a variety of pros and cons, the objective is to choose a model best suited for regeneration of damaged cortex in the mouse. Of the models of focal ischemic injury available, three of the most widely used models are MCAO, photothrombotic ischemic injury, and ET-1 induced ischemic injury.

MCAO is a technique which involves occluding the middle cerebral artery usually with nylon thread of a specific diameter. This thread is inserted into the common carotid artery, and pushed through the internal carotid artery until it occludes the middle cerebral artery. The thread can be withdrawn at any time, depending on the size and extent of ischemic injury desired (Engel et al., 2011). As the volume of brain supplied by the middle cerebral artery is quite large, encompassing much of the striatum and

Figure 1.4   Electroporation of the Adult Subventricular Zone   Plasmid DNA is injected into the lateral ventricle (black) as depicted by the needle track (blue hashed line). Electrodes are placed on either side of the head, with the positive electrode on the side of injection. An electric pulse (orange arrows) forces DNA into cells on the lateral side of the ventricle which express a fluorescent protein marker (depicted in green).
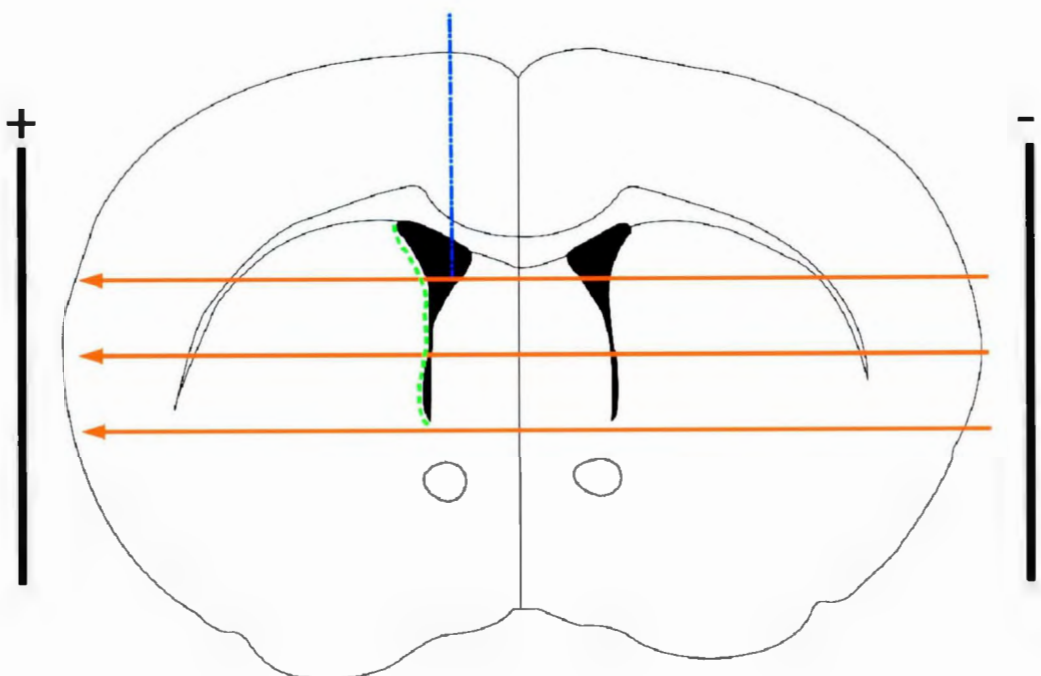
Figure 1.4

overlying cortex, the size of the injury tends to be large as well. Additionally, backflow via leptomeningeal collateral arterioles into the middle cerebral artery territory can reduce ischemic damage. The leptomeningeal collateral network is variable between animals and can produce unwanted variability. Additionally, mouse strains with more collaterals are more resistant to MCAO induced ischemic injury (Zhang et al., 2010).

Photothrombotic ischemic injury is an injury whereby a systemic photosensitive dye (rose-bengal) is stimulated to produce molecular oxygen, which stimulates fibrin clot formation (Watson et al., 1985). The dye is activated by illuminating the cortex with arc-lamps filtered to 560nm light, or a laser, which can target a precise region of the cortex based on where it is shone. While this model is precise and can produce small targeted infarcts, there is significant overhead cost involved with purchasing laser equipment and dyes.

ET-1 ischemic injury involves injecting ET-1, a vasoconstrictive peptide, into a desired location where it produces an ischemic injury by occluding local vasculature. ET-1 produces a small precise injury, given the overhead costs of a stereotaxic surgery apparatus and the peptide itself. The surgical equipment for ET-1 injections alone is more cost-effective than equipment required for photothrombotic ischemic injury as it obviates the need of expensive laser equipment.

Table 1.2: Comparing ischemic injury models

Injury Type	MCAO	Photothrombosis	ET-1
Cost	Low	High	Low
Infarct Size	Large striatal/cortical	Small & precise	Small & precise

From Table 1.2, the benefits of using ET-1 ischemic injury for a model of cortical ischemia are clear. It produces a small targeted infarct, which makes damage to the NPCs avoidable. Producing a small infarct may facilitate more complete regeneration of the infarct. As well, the overhead costs are lower than those associated with photothrombotic injury. As stereotaxic surgery is a widely popular technique, the apparatus required for

ET-1 ischemic injury may already be available in local research facilities.

As there is a great reservoir of transgenic mouse strains, as opposed to rats, there are many regenerative therapies that would only be possible to test in these mouse strains. However, there are very little data comparing behavioural tests to small cortical ischemic injuries in the mouse. A variety of research projects can take advantage of a model of ET-1 induced cortical ischemia in the mouse, where behavioural tests can be used to predict the injury. While ET-1 requires study in its role in mouse cortical ischemic injury models, its pharmacological properties have been studied extensively, strongly supporting its use in a model of ischemic stroke.

1.4.2 - ET-1 induced cortical ischemia

ET-1 is a 21 amino acid, soluble, vasoactive peptide which can produce ischemic CNS lesions. Endogenously derived from vascular endothelial cells throughout the body, ET-1 is a mediator of smooth muscle tone in the vasculature. ET-1 acts on smooth muscle and endothelial cells adjacent to where it is released (Davenport, 2002).

ET-1 can act as a vasoconstrictor or a vasodilator, based on which receptor subtypes it interacts with. Endothelin-receptor subtype A (ET-A) is found on smooth muscle and induces it to contract inducing vasoconstriction. In contrast, endothelin-receptor subtype B (ET-B) is found on endothelial cells and activates nitric oxide synthase resulting in nitric oxide release (Davenport, 2002). Nitric oxide diffuses through cell membranes and activates guanylate cyclase in smooth muscle cells (Derbyshire & Marletta, 2009). Guanylate cyclase produces cyclic GMP, signals myosin light chain kinase dephosphorylation in smooth muscle and, subsequently, prevents smooth muscle contraction (Surks, 2007). While ET-1 can have opposing effects on the vasculature in the brain, vasoconstriction is the net response when applied exogenously.

Local application of ET-1 *in vivo* can produce vasoconstriction lasting long enough to induce ischemic tissue damage. In particular, ET-1 can be used to induce an ischemic lesion in the CNS. In rats, this has been demonstrated by injecting ET-1 intra-striatally (Fuxe et al., 1992) and intra-cortically (Windle et al., 2006). Similarly, in the

26

mouse. ET-1 can induce an ischemic lesion by intra-cortical injection or by injection into subcortical white matter (Sozmen et al. 2009; Tennant et al., 2009; Wang et al., 2007b). However, these injections produce small lesions local to the site of injection, and are much smaller in size than ET-1 induced lesions in rats (Windle et al., 2006).

The size of ET-1 induced lesions in mice may be due to the profile of ET-1 receptors in the mouse brain. The degree to which the cortical vasculature responds to ET-1 is related to the ratio of ET-A to ET-B receptors. In mice, the ET-A:ET-B ratio is lower than in rats (Wiley & Davenport, 2004) and may therefore account for smaller infarct sizes in mice. As ET-B receptor activation leads to nitric oxide synthase activation, L-NAME, a nitric oxide synthase inhibitor, has been shown to increase lesion size and behavioural deficits on a forelimb motor task in mice when co-injected with ET-1 in the cortex (Horie et al., 2008). This demonstrates the role that ET-B receptors play in mitigating ET-1 mediated ischemic injury. Horie and colleagues initially found no infarcts using intra-striatal ET-1 injections, but found infarcts when ET-1 was co-injected with L-NAME. The reason that no infarcts were initially discovered may have been due to their sectioning protocol: they used 2mm thick sections instead of 20 & 50µm thick sections in which small ET-1 mediated infarcts are easily distinguished (Wang et al., 2007b, Tennant et al., 2009, Sozmen et al., 2009). This suggests that an infarct may have been produced but the thickness of the sections was inappropriate to analyze the infarct. Despite the size of ET-1 mediated infarcts being smaller than those in rats, they do occur and there are multiple studies demonstrating consistent injuries in mice (Wang et al., 2007b, Tennant et al., 2009, Sozmen et al., 2009). ET-1 is, therefore, a useful tool to produce ischemic injury in the mouse cortex, white matter and striatum, reliably producing a small focal injury.

A major limitation of previous studies using ET-1 to target the mouse forelimb motor cortex (FMC) is that the FMC was not previously mapped in detail. The standard map for the mouse motor cortex has been the Mouse Brain Atlas (Franklin & Paxinos, 2004) which uses rat cortical motor maps to infer the location of the mouse motor cortex (Zilles, 1985, Fig. 1.5, red shaded area). However, recently the mouse FMC has been specifically mapped. This was done by stimulating the cortex in a grid pattern using

micro-electrodes and observing the corresponding motor response (Tennant et al., 2011, Fig. 1.5, green shaded area). The core of the FMC includes an area of cortex where stimulation elicits a forelimb response 80%-100% of the time (Fig. 1.5, dark green shaded area). Outside this area, stimulation elicits forelimb motor responses less than 80% of the time — at the edge of the FMC, stimulation elicits a forelimb response less than 20% of the time. Because the ET-1 induced ischemic lesion is so small in the mouse cortex, studies which did not directly target the core of the FMC with ET-1 injections may have seen poor or no behavioural deficits. Behavioural tests, such as the Rota-rod and horizontal ladder have traditionally been used to assess changes in gait, but have been shown to predict FMC injury in mice (Farr et al., 2006). As Wang & colleagues' (2007) injections were anterior to the forelimb region, it is understandable that they saw only a transient impairment on the Rota-rod test at 1h post-surgery which did not persist at 3 days post-surgery. As well, Tennant & colleagues (2009) saw meagre impairments on behavioural tests: mice tested on the horizontal ladder only had deficits up to 2 days post-surgery, which resolved thereafter; cylinder tests (discussed in section 5.2) showed no deficits at all. By attempting to ablate the core of the FMC with an ET-1 induced ischemic lesion using the recently available map, development of an injury model with less variability and more robust behavioural deficits may be possible, in contrast to previous studies.

1.4.3 Behavioural testing in mouse models of cerebral ischemia

Research into how behavioural scores correlate to ET-1 mediated ischemic injury is valuable — predicting cortical injury can allow better assessment of the extent of injury and the extent of functional recovery after therapy. When targeting the FMC with an ischemic injury, only behavioural tests pertinent to the region of injury should be used. The cylinder test of forelimb asymmetry and the mouse staircase test are two tests of forelimb motor function which are currently employed in mouse models of ET-1 mediated ischemic injury in the cortex.

The cylinder test (Schallert et al, 2000) of forelimb asymmetry is a measure of

Figure 1.5 Motor maps of the adult mouse brain. Overlaid on a transverse view of the adult mouse brain are two maps. The positive end of the vertical axis represents the anterior end of the brain. The motor map according to Franklin & Paxinos (2004) is depicted in red hashed lines. The forelimb motor map according to Tennant et al (2011) is depicted in light and dark green hashed lines. The light green area represents the FMC whereby >5% or more of cortical electrode stimulations resulted in forelimb motor movement. The dark green area represents the FMC whereby 80-100% of cortical electrode stimulation resulted in forelimb motor movement.
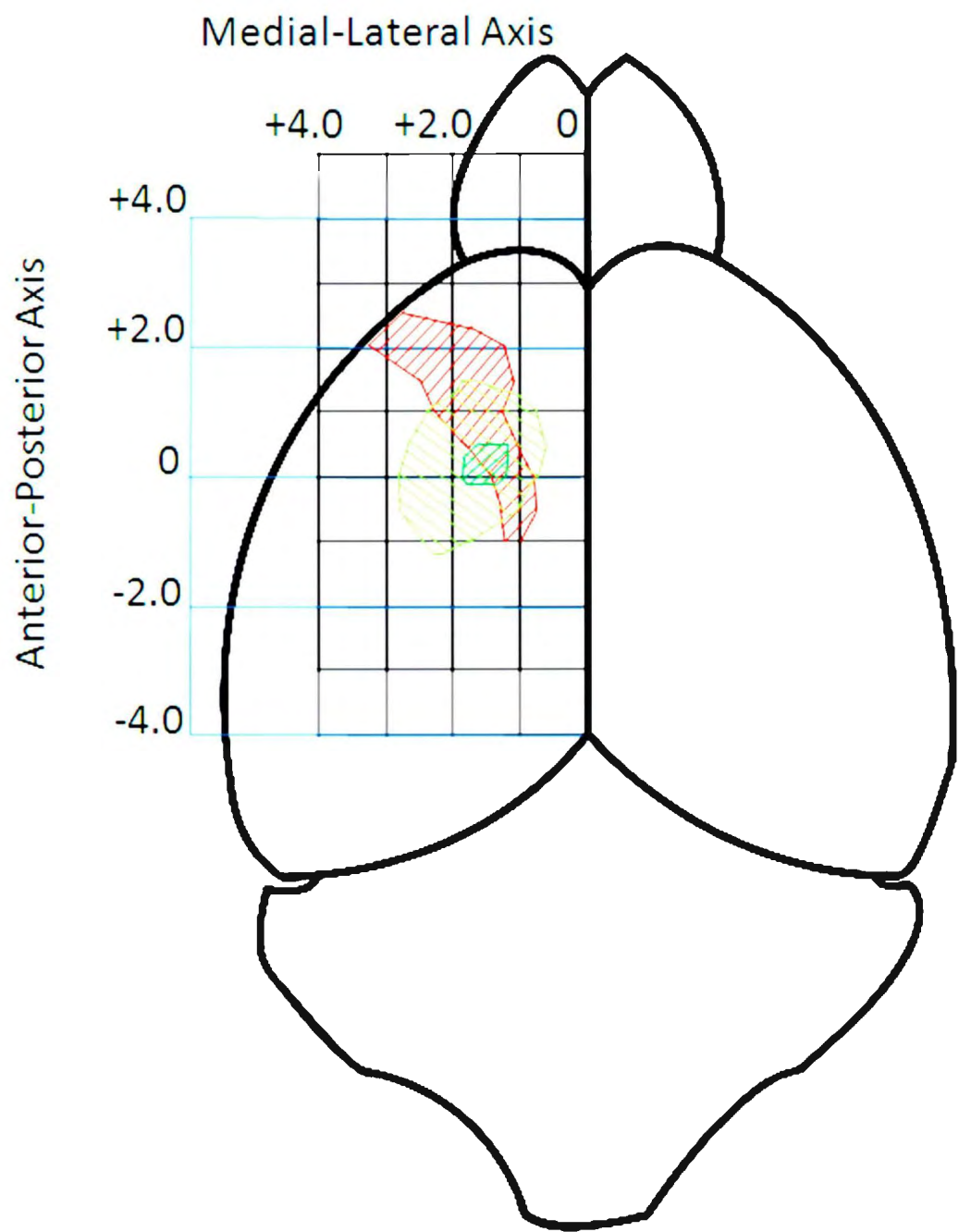
Figure 1.5

gross forelimb motor control which has recently been adapted for use in mice (Baskin et al., 2003). Mice use their forelimbs to support themselves while rearing; such supportive movements do not require dextrous reaching but do require coordinated use of their forepaws and limbs. Mice explore a translucent cylinder by rearing against the walls (Fig 2.2); the proportion of left vs right paw contacts is then quantified. In the event of unilateral FMC injury, a deficit in paw contacts contralateral to the injured hemisphere is observed. After MCAO, such deficits can be measured soon after injury (1-14 days post-injection) but resolve without treatment from 3 weeks post stroke onward (Schallert et al., 2000). Similarly, Windle & colleagues showed that deficits on the cylinder test attenuated between 1 and 4 weeks post-MCAO in rats. Though ET-1 induced cortical injury also presented a cylinder deficit at 1 week, a reduced but significant deficit was still present at 4 weeks post-injury (Windle et al., 2006). The cylinder test may, therefore, have predictive value in a model of ET-1 induced cortical injury in the mouse, even with long-term assessments.

The mouse staircase (Baird et al., 2001), adapted from the original rat staircase (Montoya et al., 1991), is a behavioural test examining forelimb motor function. This test specifically analyzes fine motor skills involved in reaching and grabbing with the forelimb in comparison to the cylinder test. Mice learn to reach pellets placed on staircases on either side of a central beam supporting the mouse (Fig 2.1). Severity of forelimb motor cortical injury is associated with fewer pellets retrieved by the limb contralateral to the injury. This test has been shown to predict cortical injury with high accuracy following cortical aspiration injury in the mouse (Baird et al., 2001) and in the rat (Montoya et al. 1991). Furthermore this test has predictive value for rat forelimb motor function after intra-cortical ET-1 induced ischemic injury (Windle et al., 2006). Due to its success in predicting cortical injury, the staircase should be tested with ET-1 induced cortical injury in the mouse.

These tests have been investigated and successfully adapted for mice; furthermore, they are reliable predictors of injury to the FMC (Baird et al., 2001, Baskin et al., 2003). These tests will be used to predict ET-1 induced FMC injury in the mouse. Using the same behavioural tests to observe reduction of deficits under treatment

conditions, regeneration of damaged tissue and functional recovery may also be assessed.

Rationale:

ET-1 has been successfully used in mice to induce ischemic stroke damage to the cortex. Despite this, there are issues with the variability of injuries, with some studies reporting no injuries at all. Therefore, demonstrating that ET-1 can produce consistent cortical infarcts is crucial to developing a model of focal ischemic injury in the mouse. Behavioural tests must then be calibrated so that behavioural deficits correlate with damage to a specific area of the cortex. Though mouse staircase and cylinder tests correlate with motor cortex injury in other models of CNS injury, they have not been tested in ET-1 induced cortical infarcts, which should be done. Furthermore, though ET-1 has been shown to produce cortical ischemic injury in the mouse, the histological parameters concerning dimensions, depth, location and volume of injury have not been correlated with behavioural deficits. I propose that assessing the mouse staircase and cylinder tests against histological parameters of ET-1 injury can further characterize the ET-1 injury model in mice. This may allow construction of inclusionary criteria for future experiments, based on the mouse staircase and cylinder tests.

Additionally, although SVZ NPCs proliferate in response to an ET-1 induced cortical ischemic injury, it remains to be determined whether neuroblasts migrate toward a focal ischemic injury in the cerebral cortex (Wang et al., 2007b). By investigating the numbers and location of Dcx+ neuroblasts post ischemia, I will assess the ability of a focal ischemic lesion to induce neuroblast proliferation and migration.

Hypothesis 1: The staircase and cylinder tests of forelimb motor function can measure ET-1 induced cortical ischemic injury.

Aims:

A) To demonstrate that ET-1 can produce an injury in the mouse FMC.

B) To investigate whether the mouse staircase and mouse cylinder tests correlate with ET-1 injury in the FMC.

C) To demonstrate that the location of the ET-1 injury correlates with the behavioural deficit.

Hypothesis 2: ET-1 induced cortical ischemic injury can induce proliferation and migration of NPC's in the ipsilateral SVZ to the injury.

Aim: To demonstrate that NPC's in the SVZ proliferate and migrate toward the site of ET-1 injury in the mouse.

Chapter 2: Methods

2.1 - Mice

Male FVBN mice were housed on a 12 hour inverted light-dark cycle, so that behaviour could be tested during the day. Mice were given standard rodent chow and water *ad libitum*. All experiments were approved by Memorial University of Newfoundland's Animal Care Ethics Committee according to the guidelines of the Canadian Council on Animal Care.

2.2 - Stereotaxic surgery

ET-1 injections (Calbiochem, 05-23-3800) were performed on 2-4 month old mice using a mouse stereotaxic apparatus (Kopf, 308019R). Body temperature was maintained from beneath with a heating pad (Softheat, HP218-12-3P). Isoflurane (Aerrane, Baxter 02225875) was used to anaesthetize mice and was mixed with oxygen using an isoflurane vaporizer (Harvard Apparatus, 340471). Anaesthesia was induced using 5%v/v isoflurane in oxygen and maintained using 2%v/v isoflurane in oxygen. After mice were anaesthetized, the scalp was shaved and disinfected with iodine solution (Proviodine USP 10%, ZK Rougier, 00172944). A scalp incision was made in the anterior-posterior axis along the skull's midline. All injections were performed unilaterally, based on staircase test performance (described in section 2.3).

A three-dimensional coordinate system was used to landmark the injection site: the dorsal-ventral axis (DV), the medial-lateral axis (ML) and the anterior-posterior axis (AP). Coordinates were first measured at lambda and bregma and identical ML and DV coordinates at each location ensured that the head was level. The injection site was measured in relation to bregma. A hole was then bored into the skull over the injection site with an Ideal Microdrill (Cellpoint Scientific, 67-1000). A syringe pump was used to control flow rate (Chemyx Fusion 100). Injections were made using a 5 μl Hamilton syringe (7633-01) attached to polyether-ether-ketone tubing (Vici Valco Instruments) and

then to a coupler (Hamilton, 55752-01) to which a pulled glass needle (World Precision Instruments, TW100F-4) was fastened. Stereotaxic coordinates, reagent concentrations, injection volume and injection rate for each type of injection are detailed in Table 2.1.

During surgery, dehydration was prevented by administering 2ml of Lactated Ringer's solution subcutaneously. Mice were given additional Lactated Ringer's solution post-surgery if body weight dropped below 80% of pre surgery weight or if mice presented dehydration-related behaviour.

Buprenorphine (50μl, 0.02mg/kg mouse weight) was also injected subcutaneously before mice were removed from anesthetic as a post-operative analgesic.

Table 2.1: ET-1 stereotaxic injections

Number of injections	Rate of Injection	Volume per injection (concentration)	Injection Location	Coordinates (AP, ML, DV)
2	0.2μl /min	1.0μl (2.0 μg/μl)	FMC	Injection 1: 0, +1.50, -1.2 Injection 2: 0, +1.75, -1.2
3	0.2μl/min	1.0μl (2.0 μg/μl)	FMC	Injection 1: +0.4, +1.6, -1.2 Injection 2: +0.2, +1.35, -1.2 Injection 3: 0, +1.75, -1.2

A daily dose of bromodeoxyuridine (BrdU, Sigma, B5552, 100μg/g body weight) was administered intraperitoneally on post surgical days 4-8 to label proliferating cells.

2.3 - Mouse staircase test

The mouse staircase is a test of skilled forelimb reaching in mice (Campden

Figure 2.1: The mouse staircase test. Mice enter the staircase chamber (left) where they reach for food pellets placed on the steps. There is a staircase on either side of a central beam preventing mice from reaching into the left staircase with their right paw (and vice versa).

Figure 2.1

Instruments, 80301, Figure 2.1). The mouse performed the task by entering the staircase chamber and reaching for pellets on either side of a divider, separating the two staircases. Injury to the FMC (Endothelin-1) was associated with fewer pellets retrieved with the contralateral forelimb.

Mice were given food rations as opposed to an *ad libitum* diet to motivate performance during training and testing. A daily ration of 3g of standard rodent chow maintained the mouse's weight above 85% body weight. Ration size was increased to 4g if weight fell below 85%. The day prior to surgery, and until testing resumed, mice were fed *ad libitum*.

Mice were trained twice daily for a minimum of 7 days before surgery or until they retrieved a consistent number of pellets. Mice were trained to reach for 15 pellets (14mg, Bio-Serv, F05684) per staircase, baiting the bottom five steps with three pellets each. The top three steps were not baited, as mice retrieved pellets from the top three steps with their tongue alone. Reaching scores two days prior to surgery were used to evaluate which hemisphere would be lesioned: the hemisphere contralateral to the paw which consistently reached the most pellets was chosen. In mice that did not have a forepaw preference but became proficient with both, in which case the hemisphere to be injected was chosen randomly. Mice were disqualified if they reached less than eight pellets per side or if the standard deviation was greater than 1 pellet four days before surgery.

Mice were tested twice daily on 6,7,13 and 14 days after surgery. The staircase contralateral to the injury was baited with 15 pellets for testing, with the other staircase left empty. Data was only collected for the paw contralateral to the injected hemisphere. Data from days 6 and 7 were averaged and analyzed as data from week 1, while data from days 13 and 14 were averaged and analyzed as data from week 2. Data were recorded as number of pellets retrieved per total pellets baited (15 pellets) and normalized to pre-stroke retrieval.

2.4 - Mouse cylinder test and filming

This test examines gross forelimb motor deficits after FMC lesion and was used to gauge whether significant FMC injury had occurred. The test involved filming a mouse rearing and touching the side of a translucent cylinder (94mm diameter, Figure 2.2) with each paw. Mice performed without external motivation.

The cylinder was placed on a translucent table and was filmed from below for quantification. Animals were filmed for 5 minutes or until 20 touches occurred. The test was administered once per day on the day before surgery and 3, 7 and 14 days post-surgery.

2.4.1   Forelimb asymmetry analysis of the mouse cylinder test

The test was quantified by analyzing each paw touch where the mouse's palm was flat against the side of the cylinder. Touches quantified were counted as left-only, right-only or bilateral (any touch where both palms were in contact with the side of the cylinder). A shift from bilateral to unilateral touching suggested a unilateral motor cortex lesion.

Forelimb asymmetry = total ipsilateral touches / (total ipsilateral touches + total contralateral touches)

2.4.2   Paw-dragging analysis of the mouse cylinder test

An alternate analysis of the cylinder test, regarding paw-dragging behaviour, was quantified by measuring how often the mouse dragged its paw against the cylinder wall during a rear. For a mouse to exhibit a paw-drag, the paw must make contact with the cylinder wall. Then, the mouse must drag its forepaw medially and then withdraw it from the cylinder, all the while maintaining cylinder contact with the contralateral forepaw. A detailed demonstration of a paw-drag is depicted in Figure 3.10. Data were expressed as the percentage of touches resulting in a drag per total number of touches with each paw and normalized to pre-stroke paw-dragging. For all regression analysis where mice are

Figure 2.2: The mouse cylinder test of forelimb asymmetry. Mice rear against the sides of a translucent plexiglass cylinder while they are filmed from beneath.
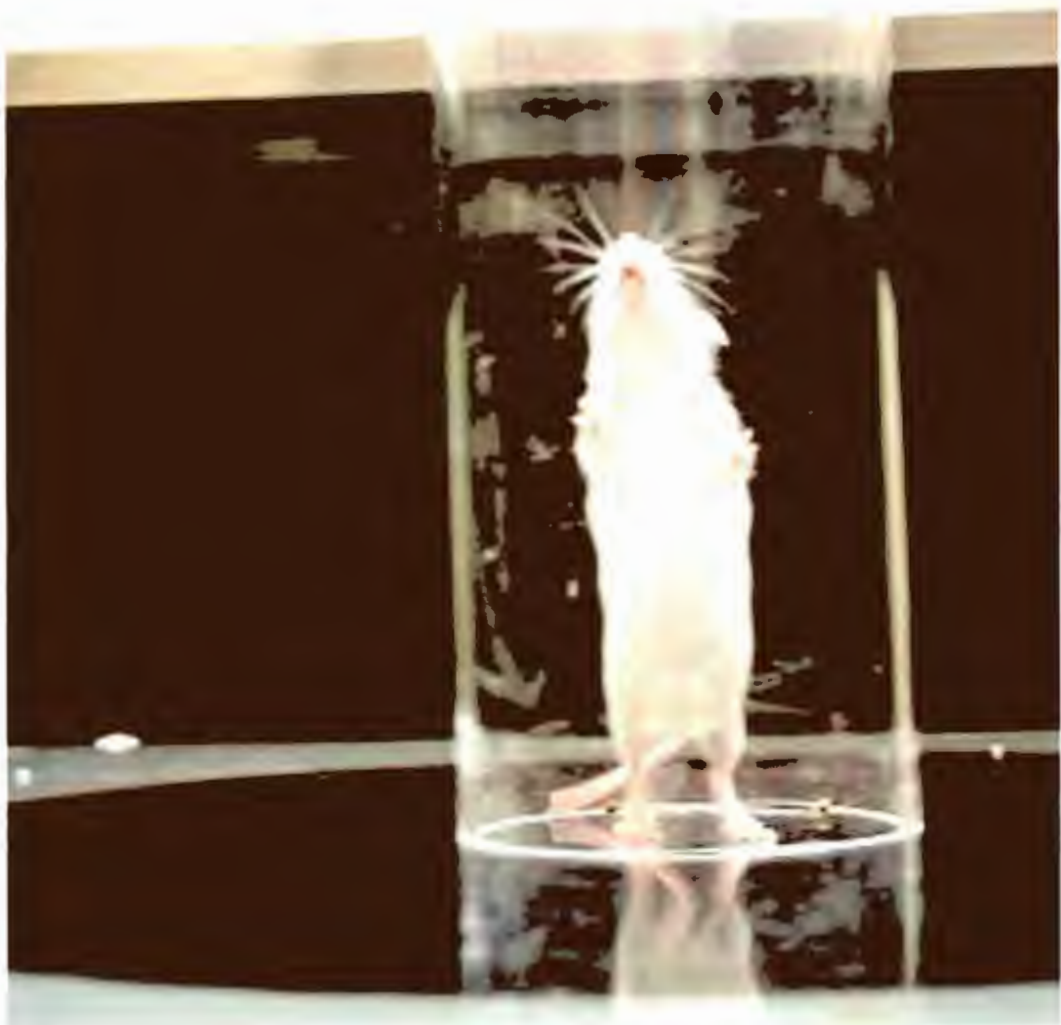
Figure 2.2

tested on the cylinder test, only data from the paw contralateral to the injection were analyzed.

2.5 - Perfusion and cryosectioning

Mice were euthanized with an intra-peritoneal injection of Euthanyl (sodium pentobarbital, 240mg/ml, CDMV 032-C). Transcardial perfusion was performed once the mouse was unresponsive. Incisions were made to expose the heart, and the right atrium was punctured to allow venous drainage. Ice cold 1x phosphate buffered saline (PBS, 137mM NaCl, 27mM KCl, 100mM Na_2HPO4, 18mM KH_2PO4, pH 7.4) (10ml) was injected into the left ventricle to flush circulating blood, followed by 20 ml ice cold 4% paraformaldehyde (PFA, pH 7.4) as a fixative. Following perfusion, the brain was removed from the skull and post-fixed in 4% PFA for 24h.

After post-fixation, brains were cryoprotected in increasing concentrations of sucrose (12, 16, 22% w/v in 1x PBS), then stored in 22% sucrose at 4°C until they were ready to be frozen.

Brains were frozen in Tissue Tek O.C.T compound (Sakura Finetek, 25608-930) using 2-methylbutane on dry-ice, held at -80°C for at least 30 minutes then equilibrated to -24°C in the cryostat for 45 minutes prior to sectioning. Sections were collected at 14μm thickness across a series of six slides (Superfrost Plus, Fisherbrand, 12-550-15), with three sections per slide. Slides were stored at -80°C until used.

2.6 - Immunohistochemistry

Slides were warmed to 37°C for 15 minutes and a hydrophobic moat was drawn around the tissue to retain antibody solution (Dako Pen, Dako, S200230-2). For BrdU immunohistochemistry (IHC), slides were post-fixed in Acetone (Fisher Scientific, A94904) for one minute. Slides were then treated with 2N hydrochloric acid for 30 minutes at 37°C to denature DNA, followed by 0.1M Sodium Borate (pH 8.0) for 10 minutes.

Primary antibodies included α-Doublecortin (for neuroblasts, 1:100, Santa Cruz Biotechnology, sc-8066), α-BrdU (1:100, BD Biosciences 347580), α-Neuronal Nuclei (for cortical neurons, 1:500, Millipore, MAB-377) and α-Cux1 (for layers II-IV cerebral cortical neuronal nuclei, 1:500, Santa Cruz Biotechnology, sc-13024). Slides were incubated with a primary antibody overnight at room temperature. The following morning, slides were incubated for 1h with the appropriate secondary antibody (1:200 donkey anti-goat IgG (H+L) Alexa Fluor 488 – Invitrogen, A11055, 1:200 donkey anti-mouse IgG (H+L) Alexa Fluor 594 – Invitrogen, A21203, 1:200 donkey anti-mouse IgG (H+L) Alexa Fluor 488 Invitrogen, A21202, and 1:200 donkey anti-rabbit IgG (H+L) Alexa Fluor 488 Invitrogen, A21206). Slides were cover-slipped in 1:3 glycerol:1x PBS and stored at -20°C.

2.7 - Immunohistochemistry imaging and counting

Sections used in immunohistochemistry were photographed using Zeiss Axiovision v4.8 software with the Zeiss Imager.Z1 (upright) microscope with 10x and 20x objectives, and a Zeiss Axiocam Mrm camera. ImageJ software (http://rsbweb.nih.gov/ij/) was used for counting. Counts were expressed as total number of Dex+ or BrdU+ cells adjacent to the ventricle or migrating toward infarcted tissue. Cells were considered adjacent to the ventricle if they were within 25μm of the ventricular surface. Migration distance was measured as the distance travelled beyond this 25μm contour of the ventricle. Six consecutive sections at 140μm intervals were examined within the infarct of each mouse. The average number of Dex+ or BrdU+ cells per section was recorded. Experimenter was blinded to all experimental conditions.

2.8 - Cresyl violet stain

Slides were heated at 37°C on a slide warmer (Thermo Scientific, MH6616X1) for 15min, then stained in 0.2% cresyl violet (Sigma, C1791) for 30 minutes. The sections were then dehydrated for 30 seconds each through a series of ethanols (50%, 70%, 90%,

95% and 100% (x3)) followed by isopropanol and toluene then cover slipped with Entellan (VWR, 34172-102) and stored at room temperature.

2.9 - Cresyl violet imaging and infarct volume calculation

Cresyl violet stained slides were used to assess infarct volume. Slides were photographed at 1.6x magnification using Zeiss Axiovision v4.8 software with the Zeiss Stemi-2000 dissecting microscope and a Zeiss Axiocam Mrm camera. The volume of the infarct was assessed by measuring the cross-sectional area of the infarct on representative coronal sections, 140μm apart, through the brain. Healthy cortical tissue was measured on either hemisphere using the outline tool, and then the infarcted area was calculated by subtracting the healthy cortical tissue area on the injured hemisphere from the uninjured hemisphere. The infarct area of each section was multiplied by 140μm to get an estimate of the infarct volume. The volume calculation for each section was added to get a total infarct volume for a specific animal. Volumes were expressed as mm^3. Experimenter was blinded to all experimental conditions.

Infarct Volume   140μm x Σ (Healthy contralateral cortical area   Healthy ipsilateral cortical area)

2.10 - Depth mapping

Depth maps were constructed using representative cresyl violet stained coronal sections, 140μm apart, through the brain. The depth of injury extending from pia to the corpus callosum was measured in 250μm "bins", throughout the medial-lateral extent of each section. An injury extending down to the corpus callosum was given a value of 100%; otherwise depth was expressed as a percentage of damaged cortex. A 140μmx250μm grid was overlaid on Tennant & colleagues' map of the FMC. Overlap with the 80-100% core, 60-100% core and the entire forelimb motor area in general was calculated by noting which bins overlapped with each respective area of the FMC. These

values were recorded as percentages.

2.11   Statistics

All statistics were performed using GraphPad Prism 5 software. Mice were tested on the staircase test twice daily with each time point representing the average of four tests across two days (1 week staircase scores are the average of two tests on days 6 and 7, respectively).

Infarct coverage of the FMC was compared to mouse staircase, cylinder and paw-dragging behaviour with linear regression analysis to determine whether there was a correlation between the coverage of the FMC and deficit severity. For each mouse, the number of orange and red coloured bins, representing deep cortical infarcts, were counted and expressed as a percentage of the total number of bins in the 80-100%, 60-100% and 40-100% regions of the FMC. For linear regression analysis, each mouse had a corresponding data point at each time point tested on the staircase, cylinder and paw-dragging tests respectively.

To test whether the location of the infarct and the time post-surgery could affect the severity of staircase deficits, these variables were compared with a two-way repeated measures analysis of variance (ANOVA). Data from the mouse staircase were compared within time points (7 and 14 days post-surgery) and between groups (OFF-target saline, ON-target saline, OFF-target ET-1, ON-target ET-1) using two-way ANOVA followed by Bonferonni's post-hoc analysis. Using data obtained from regression analysis comparing staircase deficits to infarct coverage of the anterior FMC, staircase data was separated into two groups — animals which had an injury which was "ON-target" and those which had an injury which was "OFF-target". To separate the data, ET-1 injected animals were identified as having an ON-target infarct if at least 20% coverage of the anterior FMC_{40-100} was covered with orange or red bins. Those with less than 20% coverage were deemed OFF-target. To demonstrate that the location of injury from saline injections did not affect staircase deficits, two criteria were made for being classified as ON-target: first that the majority of the injury fell within the anterior FMC_{40-100} and, if not, at least 30% coverage

of the FMC_{40-100} with any depth of injury was required.

To test whether the location of the infarct and the time post-surgery could affect the extent of forelimb asymmetry and paw-dragging, these variables were compared with a two-way analysis of variance. Data from forelimb asymmetry and paw-dragging analysis were compared within time points (before, 3, 7 and 14 days post-surgery) and between groups (saline affected paw, saline unaffected paw, ET-1 affected paw, ET-1 unaffected paw) using two-way repeated measures ANOVA followed by Bonferonni's post-hoc analysis.

To determine whether there was a difference in the number of Dex+ cells between the contralateral and ipsilateral SVZ to the infarct, Dex+ cell counts were analyzed by an unpaired t-test. To determine the difference in migrating Dex+ cells between the contralateral and ipsilateral corpus callosum and cortex to the infarct, a two-way ANOVA followed by Bonferroni post hoc tests was used. Data were compared between hemispheres (contralateral vs ipsilateral) and within maximum migration distances (up to 150µm, >150µm - 300µm, >300µm - 450µm or >450µm - 600µm). Significance was assessed at $p < 0.05$ for all statistical tests.

Chapter 3: Results

3.1 - ET-1 induces ischemic injury in the mouse cerebral cortex

To test whether ET-1 can create a reproducible infarct, ET-1 was injected twice into the FMC. During preliminary testing with FVBN mice, 1μg/μl concentrations of ET-1 produced very small infarcts when injected intra-cortically (data not shown). Two injections were made using a relatively high concentration of ET-1 (2μg/μl) to ensure that the infarct was large enough to produce behavioural deficits. Cresyl violet stained sections obtained 2 weeks post-surgery were analyzed. Healthy tissue exhibited large neuronal cell bodies easily resolved by the cresyl violet stain (Fig 3.1A,B) (Lipton, 1999). Mice receiving a saline injection had pale cresyl violet staining near the surface and in the vicinity of the injection site. Sparse condensed cell bodies which appeared dark from cresyl violet staining suggested mechanical damage from the needle puncture (Fig 3.1C,D). In contrast, mice receiving ET-1 injections had broad infarcts often extending from the pia to the dorsum of the corpus callosum. The majority of the infarct was marked by an increase in small cell bodies, which stained darkly with cresyl violet. The border of the infarct had pale cresyl violet staining with sparse condensed cell bodies, similar to that observed with mechanical damage in the saline injected mice (Fig 3.1E,F). This demonstrates that two ET-1 injections produce a large ischemic injury in the mouse cerebral cortex which can be distinguished by cresyl violet histology.

To quantify the size of the infarct, the volume was measured and compared to the damage observed in saline injected control mice. The mean volume of damaged tissue in saline injected mice was $0.42 \pm 0.08mm^3$. In comparison, the mean volume of damaged tissue in ET-1 injected mice was nearly three times larger at $1.43 \pm 0.17mm^3$ (Fig 3.1G). The ET-1 induced infarct volume is consistent with Tennant & colleagues' study demonstrating a mean volume near $1.0mm^3$ in mice (Tennant et al., 2009). The next set of mice was given three injections of saline or ET-1 to assess the effect of a larger injury size on behavioural deficits. The mean volume of damaged tissue in saline injected mice was $0.34 \pm 0.13mm^3$ compared to $2.55 \pm 0.21mm^3$ in ET-1 injected mice   greater than

Figure 3.1: ET-1 produces a significant infarct volume in the mouse cerebral cortex.

(A, C, E) Representative photomicrographs of cresyl violet stained brain sections from a control no-injection mouse, a saline injected mouse and an Endothelin-1 injected mouse respectively.

(B, D, F) High magnification photomicrographs from A, C and E respectively (black rectangles).

G) Quantification of infarct volumes between saline injected mice and ET-1 injected mice at 2 weeks post-injection, for two and three-injection groups. Data are expressed as mean ± SEM (mice receiving 2 injections, n=16 saline, n=25 ET-1, mice receiving 3 injections n=12 saline, n=15 ET-1, ***p<0.0001).

A No injection B

C Saline D

E Endothelin-1 F

2000 µm

1000 µm

G

Infarct Volume (mm^3)

Saline
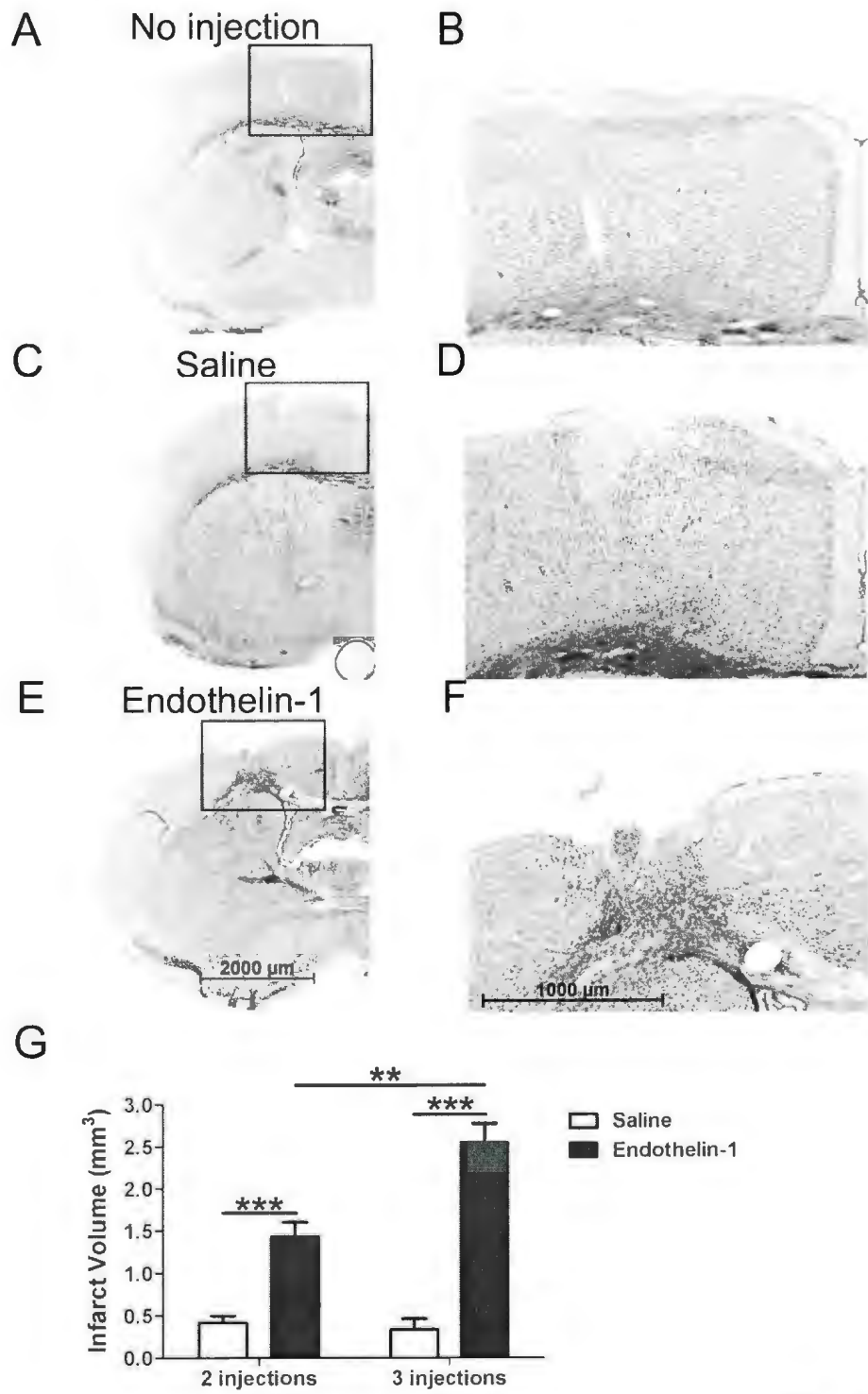Endothelin-1

2 injections   3 injections

**
***
***

Figure 3.1

the injury induced in the 2-injection group. Together these results suggest that ET-1 produces an easily identifiable infarct in the mouse brain which is significantly larger than mechanical damage associated with a saline injection.

3.2 - ET-1 infarcts produce a deficit in the mouse staircase test when targeted to the FMC.

Further tests were performed to determine if ET-1 induced infarct targeted to the motor cortex can produce measurable behavioural deficits. The mouse staircase test was used here to examine reaching and grasping motions with the forelimb. Mice were given two stereotaxic injections of ET-1 in the motor cortex according to the Paxinos motor cortex map (Fig 3.2A) (Franklin & Paxinos, 2004). Mice were tested on the staircase test before injection (which served as a baseline), at 1 week and at 2 weeks post-surgery. Of these mice tested, there was no trend toward a drop in pellet reaching (Fig 3.2B). Due to the lack of an observed deficit, a refined motor map specifically for FMC was required. The FMC map developed by Tennant & colleagues was used to select two new ET-1 injection sites (Tennant et al., 2011). In contrast to the Paxinos map, the Tennant map is smaller and specifically represents forelimb motor function (Fig 3.2C). The core of the Tennant motor map represents a cortical area which, when stimulated with a microelectrode, induces a forelimb movement 80-100% of the time. Two injection sites were chosen within the 80-100% FMC core (dark green hatched area, Fig 3.2C) assuming that the core of the FMC would be crucial to executing a forelimb motor movement. Mice with ET-1 injections within this area demonstrated a consistent drop in pellet reaching with the affected forepaw at 1 and 2 weeks post-injection, as opposed to mice which had injections based on the Paxinos motor map (Fig 3.2D). After performing a two-way ANOVA examining injection site locations versus the times which they were tested, there was a significant effect of injection sites on pellet retrieval ($F_{(1,16)}$ 23.77, p<0.001, Fig. 2E). Injection sites targeting the 80-100% FMC core were used in future experiments based on their ability to induce a consistent forelimb motor deficit.

To increase the signal-to-noise ratio, future experiments used a smaller pellet size such that 15 pellets (up from 10 pellets) could be baited on the bottom 5 steps of the

Figure 3.2: ET-1 infarcts produce a deficit in the mouse staircase test when targeted to the FMC.

A) The motor cortex according to Paxinos & colleagues is represented in the hatched red area on a horizontal plane of the mouse brain (Franklin & Paxinos, 2004). The map is represented as a horizontal grid overlaid on the left cortical hemisphere, with both axes in reference to the skull landmark bregma. Injection coordinates were: a) AP+0.5, ML+1.75 and b) AP+0.9, ML+1.75. Anterior-posterior (AP), Medial-lateral (ML).

B) The graph represents the change in pellet reaching at 1 week and 2 weeks in reference to pre-stroke reaching, using injection coordinates in A.

C) Injection sites were refined according to Tennant & colleagues' FMC map (Tennant et al., 2011). The motor cortex is represented in the hatched green area on a horizontal plane of the mouse brain, with the 80-100% core hatched in dark green. Paxinos' motor cortex map is included for comparison, in hatched red. Injection coordinates are: a) AP+0.0, ML+1.5 and b) AP+0.0, ML+1.5.

D) The graph represents the change in pellet reaching at 1 week and 2 weeks in reference to pre-stroke reaching, using injection coordinates in C.

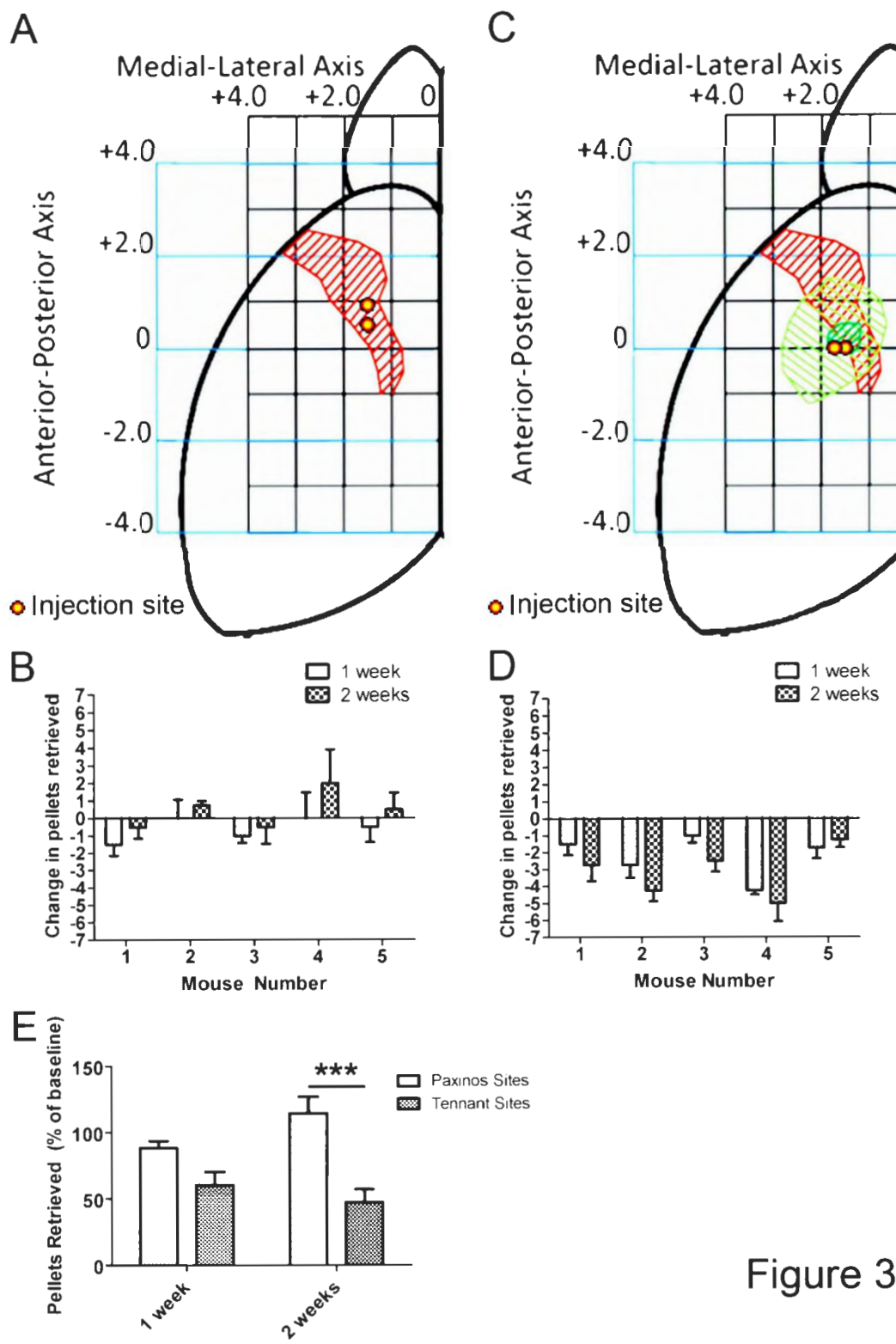E) Injection sites using Tennant's map were compared to injection sites using Paxinos' map. ***$p<0.001$

Figure 3.2

staircase (3 pellets per step, up from 2 pellets per step). The top three stairs of the staircase were not baited due to mice retrieving pellets directly with their tongue.

3.3 - The mouse staircase test correlates with location and depth of ET-1 infarcts.

After demonstrating that ET-1 can induce infarcts in the mouse cerebral cortex, ET-1 induced injury was correlated to behavioural deficits after assessing mice using the mouse staircase test. Initial data comparing staircase reaching scores between ET-1 and saline injected mice were not significantly different (data not shown). In an effort to explain why some ET-1 injected mice did not have a staircase reaching deficit, the location of the injury was mapped according to Tennant & colleagues' forelimb motor map. The medial and lateral extremes of the infarct on representative coronal sections were mapped throughout the anterior-posterior extent of the infarct. This information was then overlaid on Tennant & colleagues' forelimb motor map using the Paxinos atlas to reference anatomical features with an anterior-posterior measurement. The percent of the 80-100% FMC "core" (FMC_{80-100}, and as per Tennant et al, 2011), that overlapped with the infarct map was recorded. Coverage of the core versus staircase reaching was analyzed in a regression analysis for mice receiving two injections of ET-1 (Fig 3.3A) or three injections of ET-1 (Fig 3.3B). No significant relationship existed between core coverage and staircase reaching data, however, a downward trend in reaching was observed with a greater percent of core coverage.

Though location of infarct did not correlate with a staircase deficit, this could be a result of not taking into account information about the depth of infarct. Using only information on the area of an infarct, a broad infarct would have the same value – irrespective of whether it was shallow or deep. To test this, a depth map of the infarct was overlaid on Tennant & colleagues' forelimb motor map. The depth map was constructed by measuring the depth of infarct as a percentage of the distance from pia to the corpus callosum at 250μm intervals from the midline of the brain (Fig 3.4A). A horizontal grid was overlaid on top of Tennant & colleagues' FMC map, with bins of dimensions 140μm x 250μm. Bins were then shaded in one of five hues (blue, green, yellow, orange or red)

54

Figure 3.3: The mouse staircase test compared to infarct location within the FMC.

A) Regression analysis of infarct coverage of the targeted FMC_{80-100} core vs staircase data for mice receiving 2 injections of ET-1 at 1 week ($R^2 = 0.07223$, p = 0.2150, slope=-0.290) and 2 weeks ($R^2 = 0.1249$, p = 0.0981, slope=-0.434) (n=23).

B) Regression analysis of infarct coverage of the targeted FMC_{80-100} core vs staircase data for mice receiving 3 injections of ET-1 at 1 week ($R^2 = 0.007346$, p = 0.7523, slope=-0.086) and 2 weeks ($R^2 = 0.09201$, p = 0.2534, slope = -0.329) (n=16).
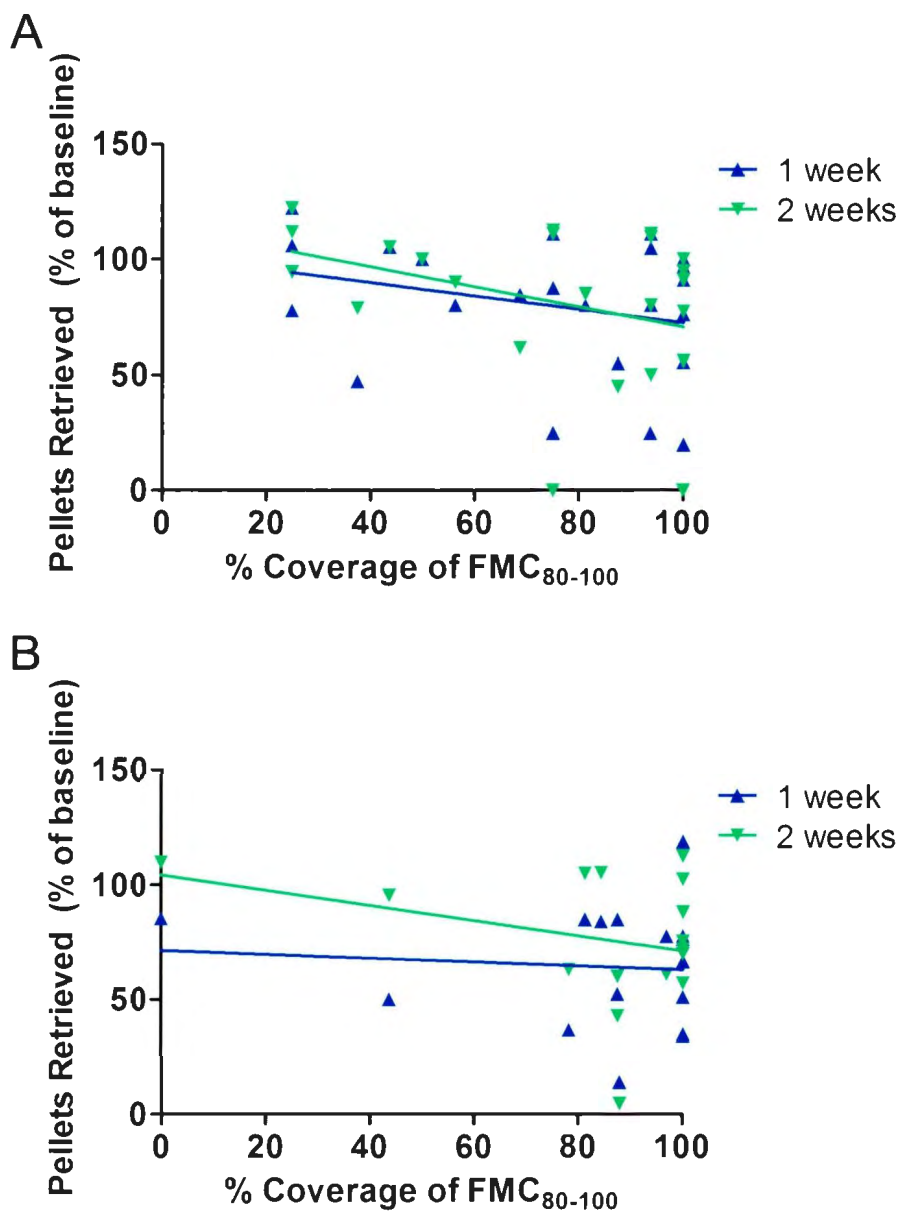
Figure 3.3

based on the percentage of cortical depth which was injured. Each of the five different hues represented a further 20% of cortical damage (e.g. red represents 80-100% of the distance from pia to the corpus callosum is damaged tissue). Saline injected mice had narrow and superficial injuries, as evidenced by the lack of red bins (Fig 3.4B). In contrast, ET-1 injected mice often had broad and deep injuries encompassing most of the FMC core (Fig 3.4C).

To accurately determine which cortical layers were affected by injuries of different depths, IHC was performed for Neuronal Nuclei (NeuN) (Fig 3.5) which labels neuronal nuclei, and Cux1 immunohistochemistry which labels neurons in cortical layers II-IV (Fig 3.5). These photos demonstrate that infarcts extending deeper than 40% of the cortex have damaged layers II-IV at those respective bins, but minimal damage to lower layer neurons was observed. Injuries extending from 60% of cortical depth and beyond (red and orange bins) will damage some layer V and VI neurons. Damage to layer V neurons may provide longer-term deficits due to the fact that they project to spinal motor neurons. By analyzing the percent of the FMC covered by orange and red bins, correlations between staircase deficits and injury location may be improved.

From this point forward, data from mice receiving either 2 or 3 injections of ET-1 were combined for regression analysis. By assuming that coverage and depth of infarct specifically within the FMC dictates deficits and not overall volume of injury, the difference between the 2 and 3 injections groups is irrelevant when asking the question: does greater coverage at greater depths correlate with behavioural deficits? Examining only ET-1 injected mice, a regression analysis was performed comparing the percent of infarct coverage of the core descending to a minimum of 80% cortical depth versus staircase reaching (Fig. 3.6A). There was no downward trend of staircase reaching observed as core infarct coverage increased at >80% cortical depth. This suggested that damaging only the 80-100% FMC core (FMC_{80-100}) is not sufficient for a lasting forelimb motor deficit. The regression analysis was then repeated, requiring the 60-100% FMC (FMC_{60-100}) to be covered by the infarct at $\geq$80% cortical depth (Fig 3.6B). A significant downward relationship in staircase reaching with greater core infarct coverage was observed at both 1 and 2 weeks. By broadening the infarct depth requirement from >80

57

Figure 3.4: Depth mapping of ET-1 infarcts.

A) Depth maps were constructed by measuring the depth of cortical injury at 250μm
intervals lateral to the midline of representative 140μm coronal brain sections using
Axiovision software.
Depth maps were overlaid on Tennant & colleagues' FMC map. Each 140x250μm "bin"
is coloured based on the depth recorded at that point.
B) Representative depth-map from a mouse with two saline injections.
C) Representative depth-map from a mouse with two ET-1 injections.

A

2001.95 μm
1749.01 μm
1499.01 μm
1249.67 μm
1001.16 μm

Legend Depth (%)
- <20%
- 20 - <40%
- 40 - <60%
- 60 - <80%
- 80 - <100%

B Saline

Legend Depth (%)
- <20%
- 20 - <40%
- 40 - <60%
- 60 - <80%
- 80 - <100%

C Endothelin-1

Legend Depth (%)
- <20%
- 20 - <40%
- 40 - <60%
- 60 - <80%
- 80 - <100%

Figure 3.4

59
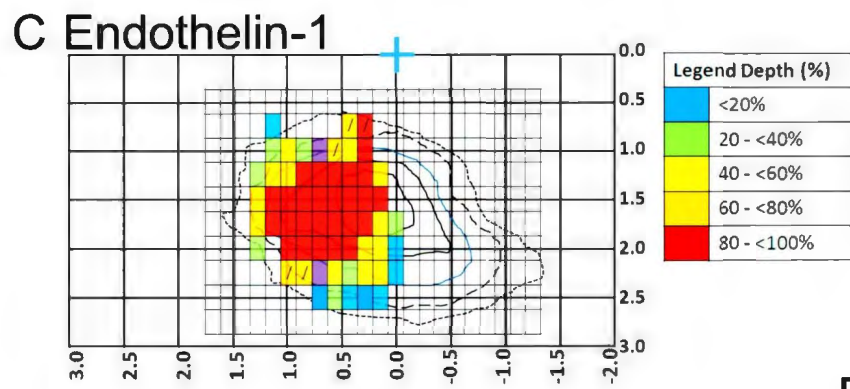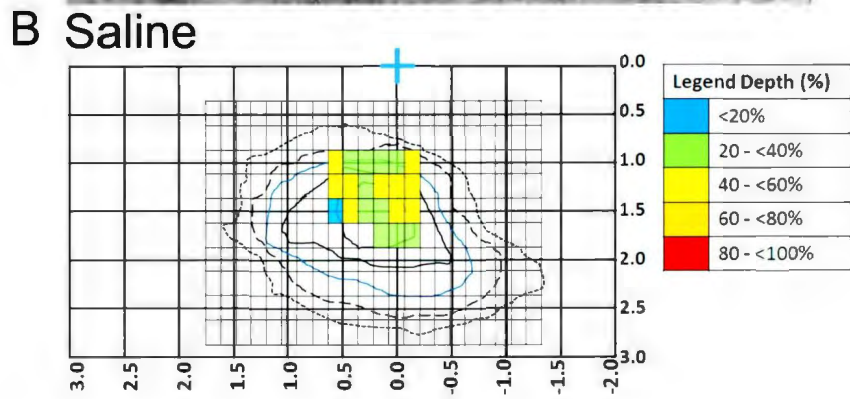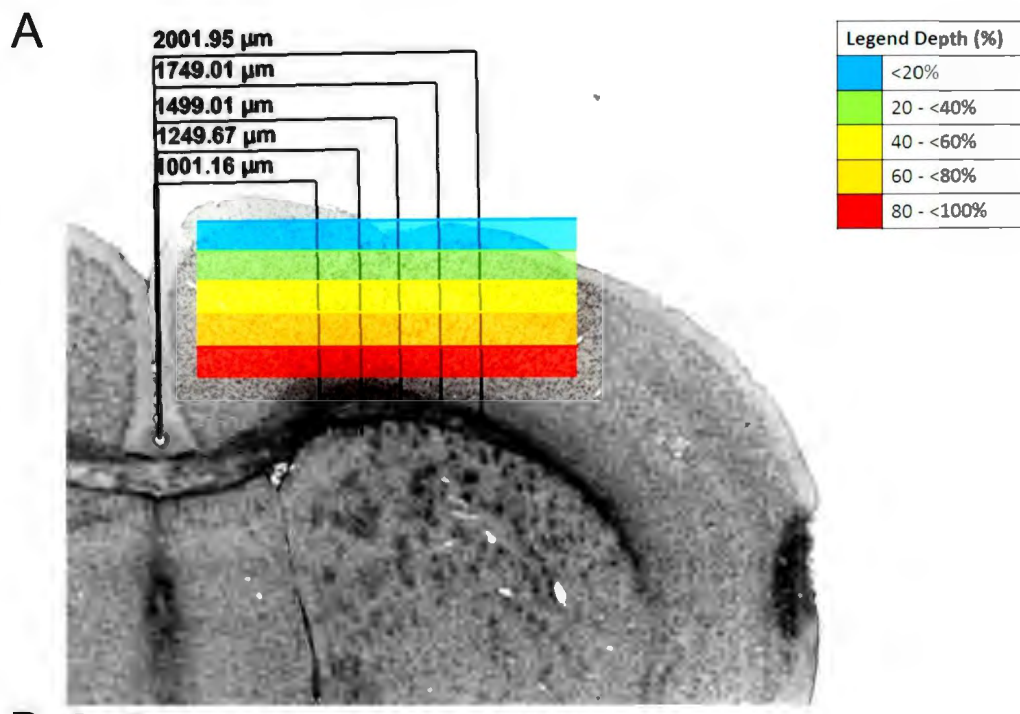
Figure 3.5: Cortical injury depth is associated with damage to specific cortical layers.

Adjacent tissue sections (140μm apart) were Nissl-stained, or stained using fluorescence immunohistochemistry directed against NeuN or Cux1. Sections were taken from representative brains with representative cortical infarct depths of <40%, <60%, <80% and 80-100%. The depth of injury and the depth of the cortex are shown on the Nissl-stained sections.
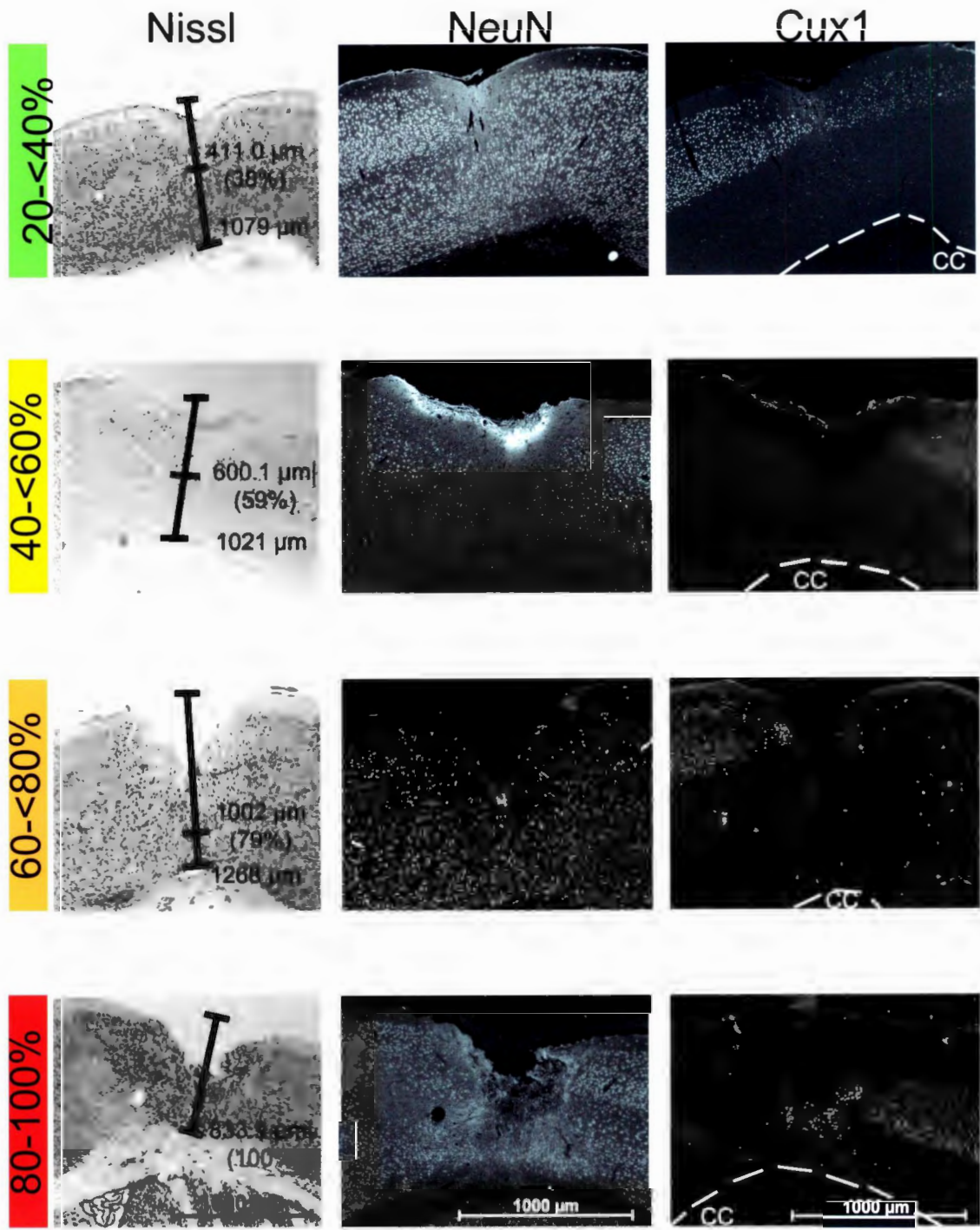
Figure 3.5

cortical depth to $\geq 60\%$ cortical depth, the trend of lower staircase reaching at greater coverage of the FMC_{60-100} became more significant at one week (Fig 3.6C). When analyzing the 40-100% FMC (FMC_{40-100}) at the same depth, the relationship was highly significant at both time points and had a stronger correlation than comparisons in the FMC_{60-100} in each case (m=-0.835 at 1 week, m=-0.860 at 2 weeks, Fig 3.6D). To examine whether the staircase test could correlate with the volume of ET-1 infarcts, a regression analysis was performed comparing infarct volume with staircase reaching scores at 1 and 2 weeks post-surgery (Fig 3.6E). This analysis showed no significant linear relationship between staircase test performance and volume of ET-1 infarct. Likewise, correlations are poor when comparing gross infarct coverage of the FMC with staircase test performance. This suggests that both the depth and location of the injury together are required to produce deficits in the staircase test.

3.4 - The mouse staircase test specifically correlates with infarcts in the anterior FMC.

While data comparing staircase performance with infarct coverage of the FMC are highly significant, the FMC is nevertheless a heterogeneous region where neurons project to spinal motor neurons and then muscles, which are involved in many different forelimb tasks. Identifying a location within the FMC which is crucial for staircase-related reaching and grasping motions may demonstrate a more significant behaviour vs coverage correlation. Recent work has demonstrated that two very large subdivisions of the FMC exist: an anterior region responsible for abductive movements, and a posterior region responsible for adductive movements (Harrison et al., 2012). The abduction may be involved in the series of movements involved in retrieving pellets in the staircase test. To analyze whether infarct coverage of the anterior FMC resulted in staircase deficits more often than similar coverage of the posterior FMC, ET-1 injected mice were assessed in relation to percent infarct coverage of the FMC_{80-100}, FMC_{60-100}, and FMC_{40-100} areas. Coverage was assessed separately for the portions of those maps which were anterior or posterior (respectively) to the line AP +0.25, which bisects the FMC into roughly equal sized anterior and posterior sections. Correlation of staircase performance

Figure 3.6: The mouse staircase test correlates with infarcts in the FMC.

A) Regression analysis of % coverage of the FMC_{80-100} at $\geq 80\%$ cortical depth of infarcted tissue vs staircase data for ET-1 injected mice at 1 week (R^2 0.040, p 0.222, slope -0.195) and at 2 weeks (R^2 0.019, p 0.398, slope -0.147) (n 39).
B) Regression analysis of % coverage of the FMC_{60-100} at $\geq 80\%$ cortical depth of infarcted tissue vs staircase data for ET-1 injected mice at 1 week ($R^2 = 0.184$, p<0.01, slope=-0.588) and at 2 weeks ($R^2 = 0.139$, p<0.05, slope=-0.552) (n=39).
C) Regression analysis of % coverage of the FMC_{60-100} at $\geq 60\%$ cortical depth of infarcted tissue vs staircase data for ET-1 injected mice at 1 week (R^2 0.129 , p<0.05, slope -0.466) and at 2 weeks (R^2 0.181, p<0.01, slope -0.598) (n-39).
D) Regression analysis of % coverage of the FMC_{40-100} at $\geq 60\%$ cortical depth of infarcted tissue vs staircase data for ET-1 injected mice at 1 week ($R^2 = 0.232$, p<0.01, slope=-0.835) and at 2 weeks (R^2 0.210, p<0.01, slope-0.860) (n-39).
E) Regression analysis of infarct volume vs staircase data for ET-1 injected mice at 1 week (R^2 0.057, p 0.1425, slope -6.912) and at 2 weeks (R^2 0.006, p 0.630, slope -2.487) (n 39). *p<0.05, **p<0.01

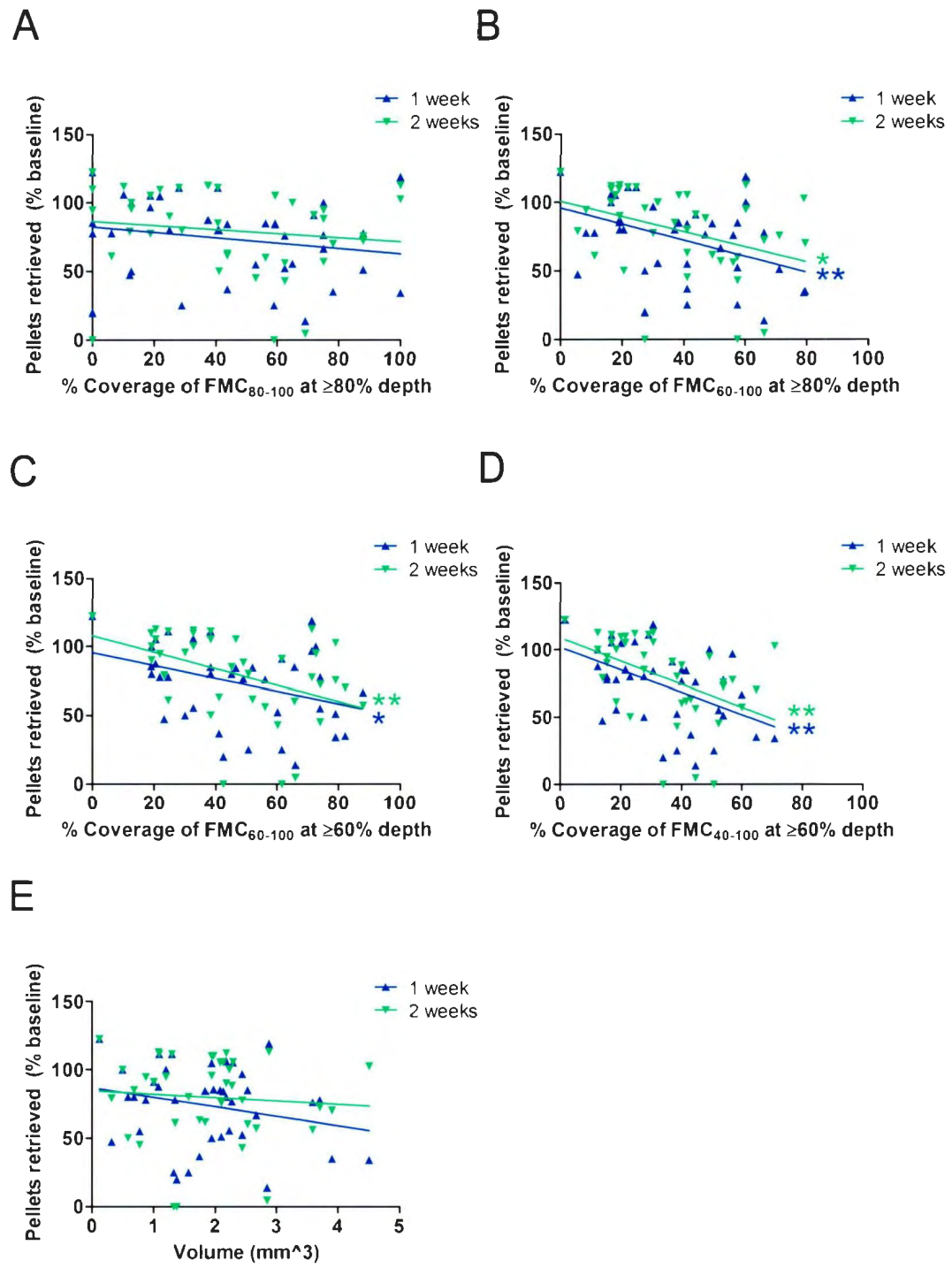Figure 3.6

with infarct coverage of the anterior FMC_{60-100} at >80% cortical depth demonstrated a remarkable significance at 1 and 2 weeks post-injury (Fig 3.7A). By analyzing FMC_{60-100} at >60% depth, the relationship was more significant and the strength of the correlation improved (m= -0.682 at 1 week, m =-0.666 at 2 weeks, Fig 3.7C). Analyzing the FMC_{40-100} resulted in a lower R^2 than the analysis of the FMC_{60-100} at both time points, but a stronger slope at 2 weeks. (m= -0.566 at 1 week, m= -0.729 at 2 weeks, Fig 3.7E). This suggests that while the FMC_{60-100} is predominantly required for staircase retrieval, the FMC_{40-100} may contribute to staircase reaching behaviour as well. Consistent with our hypothesis, regressions of staircase retrieval with coverage of the posterior FMC displayed no relationship whatsoever when analyzing the FMC_{60-100} at >80% depth (Fig 3.7B), ≥60% depth (Fig 3.7D) and the FMC_{40-100} at ≥60% depth (Fig 3.7F). We concluded that damage in anterior as opposed to the posterior FMC results in greater deficits in the staircase test.

Using data obtained from regression analysis comparing staircase deficits to infarct coverage of the anterior FMC, the staircase data was separated into two groups animals which had an injury which was "ON-target" and those which had an injury which was "OFF-target". To separate the data, ET-1 injected animals were identified as having an ON-target infarct if at least 20% coverage of the anterior FMC_{40-100} was covered with orange or red bins. Those with less than 20% coverage were deemed OFF-target. To demonstrate that the location of injury from saline injections did not affect staircase deficits, two criteria were made for being classified as ON-target: first that the majority of the injury fell within the anterior FMC_{40-100} and, if not, at least 30% coverage of the FMC_{40-100} with any depth of injury was required. While the control groups (ET-1 OFF-target, saline ON-target, saline OFF-target) did not differ from one another in terms of staircase deficits, ET-1 on- target injections differed significantly from all control groups at 1 week, but not two weeks post-injection (Fig 3.8).

3.5 - An alternate analysis of the mouse cylinder test correlates with location and depth of ET-1 infarcts.

Figure 3.7: The mouse staircase test specifically correlates with infarcts in the anterior FMC.

A) Regression analysis of coverage of the anterior FMC_{60-100} at $\geq 80\%$ cortical depth of infarcted tissue vs staircase data for ET-1 injected mice at 1 week (R^2 0.405, p<0.001, slope -0.676) and at 2 weeks (R^2 0.254, p 0.001, slope=-0.589) (n 39).
B) Regression analysis of coverage of the posterior FMC_{60-100} at >80% cortical depth of infarcted tissue vs staircase data for ET-1 injected mice at 1 week (R^2=0.015, p=0.456, slope=-0.118) and at 2 weeks (R^2=0.019, p=0.398, slope=-0.147) (n=39).
C) Regression analysis of coverage of the anterior FMC_{60-100} at >60% cortical depth of infarcted tissue vs staircase data for ET-1 injected mice at 1 week (R^2 0.449, p<0.001, slope -0.682) and at 2 weeks (R^2 0.360, p<0.001, slope=-0.666) (n 39).
D) Regression analysis of coverage of the posterior FMC_{60-100} at >60% cortical depth of infarcted tissue vs staircase data for ET-1 injected mice at 1 week (R^2 0.004, p 0.716, slope -0.053) and at 2 weeks (R^2=0.028, p 0.311, slope -0.161) (n 39).
E) Regression analysis of coverage of the anterior FMC_{40-100} at >60% cortical depth of infarcted tissue vs staircase data for ET-1 injected mice at 1 week (R^2 0.206, p<0.01, slope=-0.566) and at 2 weeks (R^2 0.278, p<0.001, slope -0.729) (n 39).
F) Regression analysis of coverage of the posterior FMC_{40-100} at >60% cortical depth of infarcted tissue vs staircase data for ET-1 injected mice at 1 week (R^2 0.000, p 0.990, slope=-0.002) and at 2 weeks (R^2=0.001, p 0.853, slope=0.037) (n 39). **p<0.01, ***p<0.001.
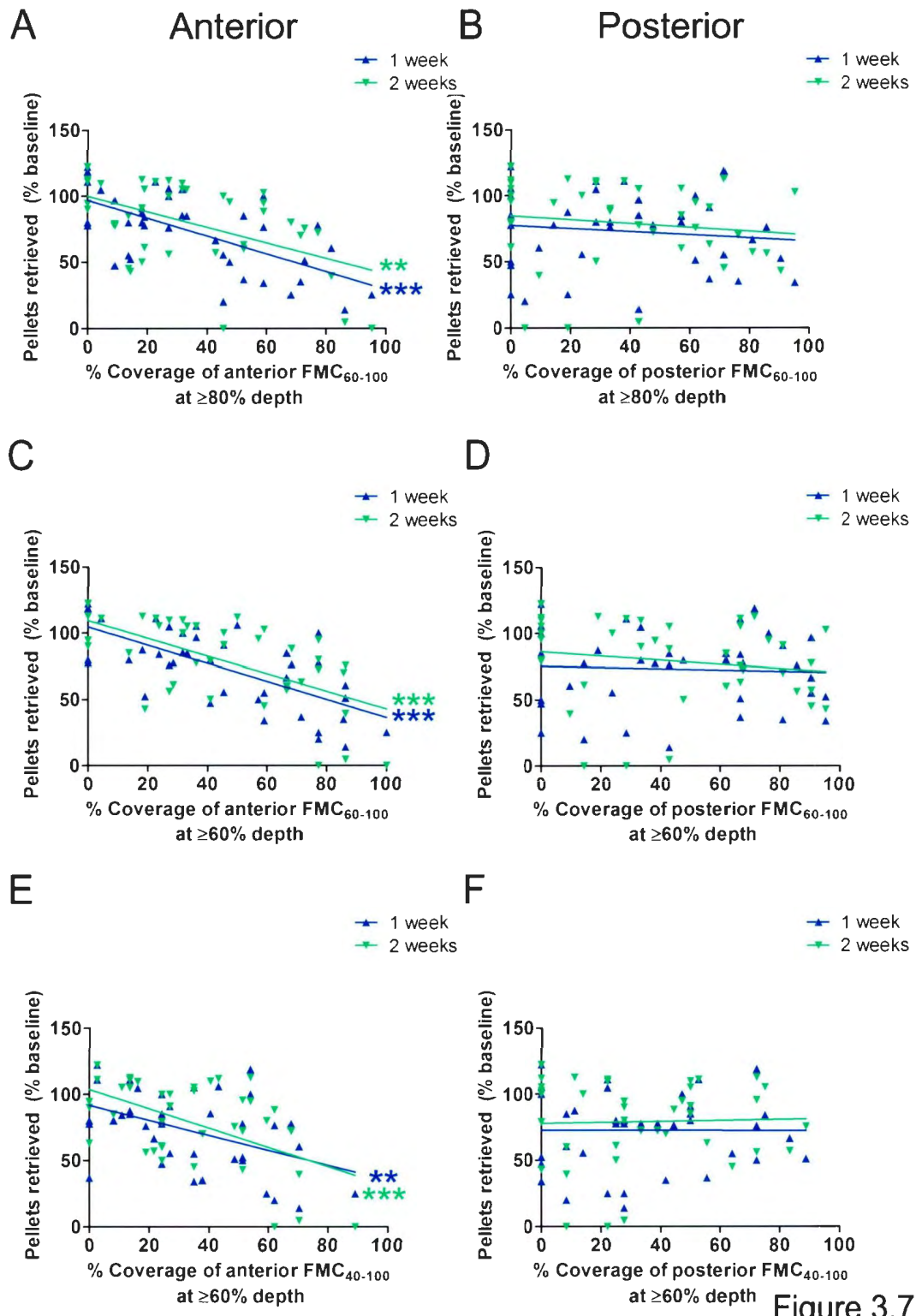
Figure 3.7

In addition to the mouse staircase test, the cylinder test of forelimb asymmetry was also used to correlate ET-1 induced ischemic injury. This test has proved successful in predicting cortical damage in rats (Schallert et al., 2000, Encarnacion et al., 2011, MacLellan et al., 2011) and in mice (Baskin et al., 2003) but has not been effective in predicting ischemic injuries induced by ET-1 in mice (Tennant et al., 2009). Overall, there was no difference in use of the affected forelimb between saline and ET-1 groups, using data from both 2 and 3 ET-1 injections (Fig 3.9A). Regressions analysis comparing forelimb asymmetry with FMC core coverage were performed on mice with both two and three injections of ET-1. Regressions on either group alone showed no significance (data not shown). There was no correlation between injury coverage of the FMC_{80-100} and a decrease in use of the affected paw (Fig 3.9B). By examining core coverage of the FMC_{60-100} using >80% depth bins only, no trend or correlation was detected (Fig 3.9C). Refining the data using >60% depth bins did not result in a trend or correlation between core coverage and use of the affected forepaw (Fig 3.9D). From these data, an ET-1 induced ischemic injury to the FMC cannot be detected using the classical cylinder forelimb asymmetry analysis.

Therefore a new analysis for the mouse cylinder test was developed. After mice rear and touch the sides of the cylinder, they push off from the cylinder wall and land on their forepaws. However, mice with ET-1 induced cortical ischemic injury tend to dismount normally with their unaffected paw, but let their affected paw-drag against the side of the cylinder toward the midline of their body as they withdraw it. This behaviour, which will be referred to as "paw-dragging" and is the basis for further cylinder analysis. Eight still frames of a video demonstrating "paw-dragging" are shown in Fig 3.10. A mouse will approach the cylinder wall (Fig 3.10A) and place one or both forelimbs firmly against the side of the cylinder (Fig 3.10B). When the mouse dismounts, it pushes against the side with both paws (Fig 3.10C) and lowers its forepaws to the ground (Fig. 3.10D). In contrast, the injured mouse will initially make contact with both forepaws (Fig. 3.10E), slightly withdraw the affected paw (Fig 3.10F) and drag the affected paw along the cylinder toward the midline of their body (Fig 3.10G) before withdrawing it from the cylinder wall entirely (Fig 3.10H).

Figure 3.8: ON-target injections of ET-1 produce significant staircase deficits.

Analysis of staircase reaching data for saline and ET-1 injected groups, separated by whether the location of the injury was inside or outside the anterior FMC (n=7 saline OFF-target, n=18 saline ON-target, n=12 ET-1 OFF-target, n=26 ET-1 ON-target). $F_{Treatment}(3,59)=4.71$, *$p<0.05$
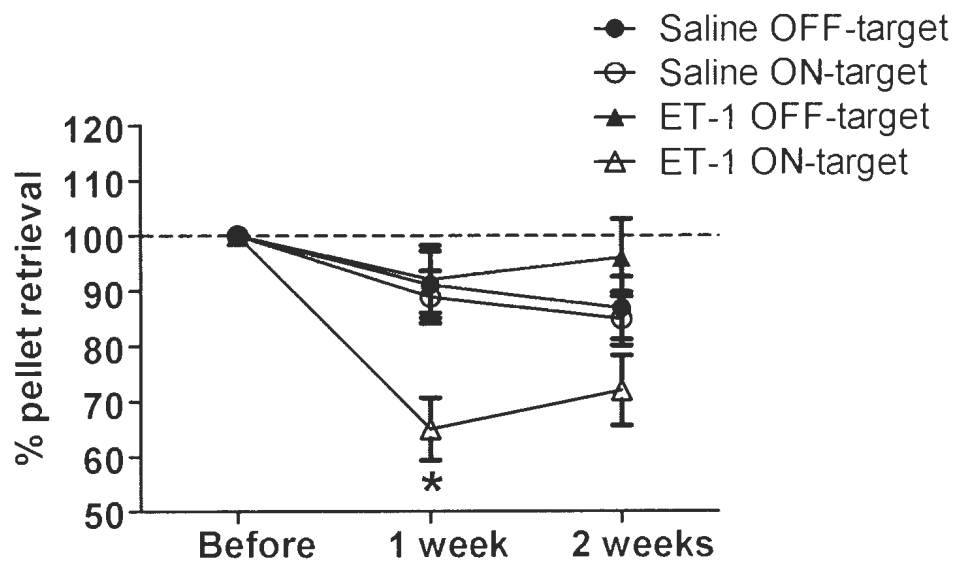
Figure 3.8

Figure 3.9: Classical analysis of the mouse cylinder test does not correlate with ET-1 infarcts.

A) Analysis of cylinder forelimb asymmetry data for 2 and 3 cortical injections. N=20 Saline, n=35 Endothelin-1.

B) Regression analysis of coverage of the 80-100% FMC core with infarcted tissue vs cylinder data for ET-1 injected mice. No significant association between injury location and paw touching with the affected paw was found at 3 days (R^2=0.000, p=0.962, slope=0.001), 1 week (R^2=0.003, p=0.733, slope=0.009) or at 2 weeks (R^2=0.017, p=0.447, slope=-0.024). (n=38)

C) Regression analysis of coverage of the 60-100% FMC core at > 80% cortical depth of infarcted tissue vs cylinder data for ET-1 injected mice. No significant association between injury location and paw touching with the affected paw was found at 3 days (R^2=0.003, p=0.734, slope=-0.010), 1 week (R^2=0.000, p=0.961, slope=0.002) or at 2 weeks (R^2=0.051, p=0.186, slope=-0.049). (n=38)

D) Regression analysis of coverage of the 60-100% FMC core at ≥ 60% cortical depth of infarcted tissue vs cylinder data for ET-1 injected mice. No significant association between injury location and paw touching with the affected paw was found at 3 days (R^2=0.001, p=0.843, slope=0.006), 1 week (R^2=0.001, p=0.891, slope=-0.004) or at 2 weeks (R^2=0.055, p=0.170, slope=-0.050). (n=38)

Figure 3.9

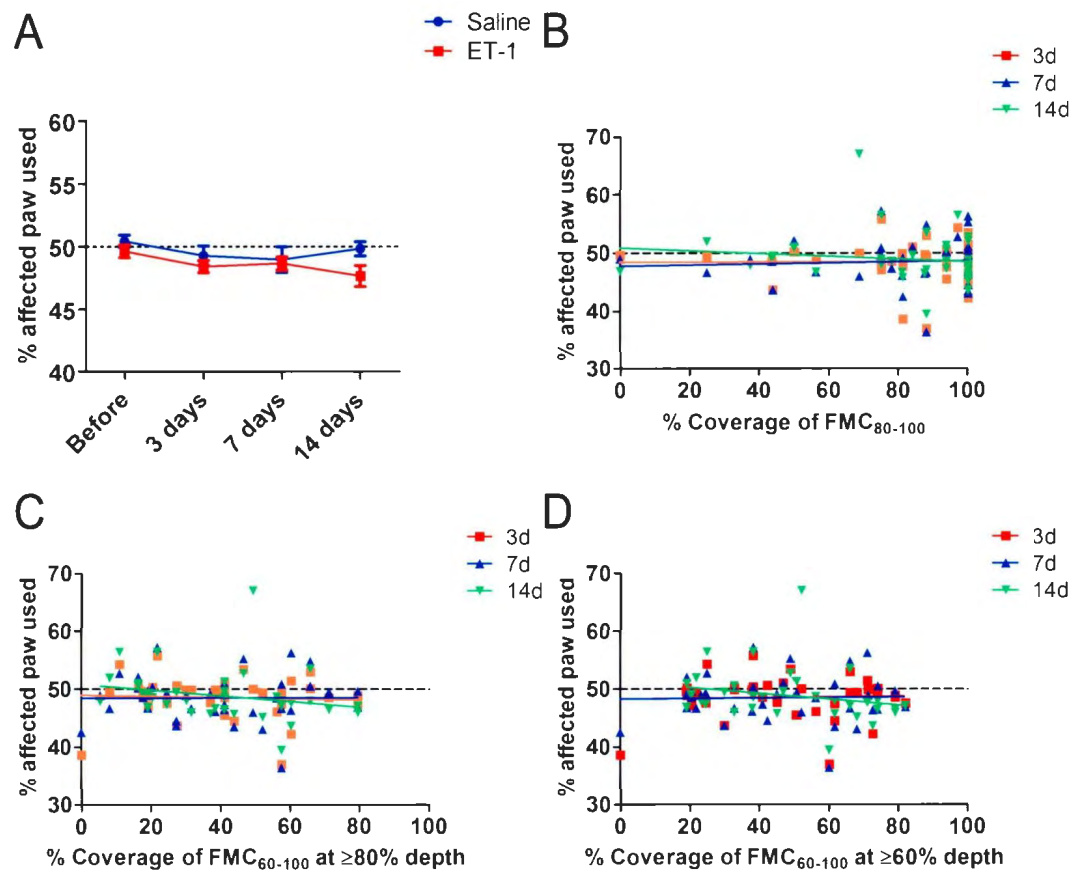Paw-dragging behaviour was quantified as a percentage of cylinder touches resulting in a paw-drag out of the total number of cylinder touches for ET-1 injected mice. Paw-dragging behaviour increased significantly at 3 days post injection following 2 and 3 injections of ET-1 (Fig 3.11A,B). While paw-dragging behaviour tends to peak at 3 days post-injection and recover thereafter, mice receiving 3 injections of ET-1 (Fig 3.11B) had a much slower recovery rate than mice receiving 2 injections of ET-1 (Fig 3.11A), with their paw-dragging behaviour remaining significantly higher than baseline at 14 days post injection. This suggests that 3-injections of ET-1 may be a better injection protocol for use in studying long-term behavioural deficits. As paw-dragging peaks at 3 days post-injection, further study should be taken to determine whether it correlates with long-term staircase deficits. This could be used as an early inclusionary criterion, allowing experimental treatments to be started sooner post-ischemia.

While paw-dragging is elevated after ET-1 injection, it is not clear whether there is a relationship between FMC damage and paw-dragging. The elevated paw-dragging may not be a result of damage to the FMC, but rather a side effect of damage to the forelimb sensorimotor cortex which abuts the FMC. Comparing paw-dragging behaviour to coverage of the FMC_{60-100} at $\geq 60\%$ depth with a regression analysis, a significant relationship emerges whereby paw-dragging observed at 3 and 14 days post-injection increases as core coverage increases (Fig 3.11C). By performing another regression analysis using coverage of the FMC_{40-100} area at $\geq 60\%$ depth, the relationship between core coverage and paw-dragging is significant at 3, 7 and 14 days post-injection, and the slopes are strongest at each time point (m=0.393 at 3d, m 0.240 at 1 week, m 0.293 at 2 weeks, Fig 3.11D).

A regression analysis was performed comparing staircase deficits at one week post-injection (normalized to pre-injection behaviour) with paw-dragging at 3 and 7 days post-injection. While there seems to be a trend at 3 days post-injection (m 0.148, R^2 0.076, p 0.12), there is a significant correlation between a deficit in staircase reaching at one week and increased paw-dragging at 7 days post-injection (m=0.126, R^2=0.145, p<0.05, Fig 3.11E). While staircase and cylinder tests both measure forelimb motor deficiency in mice, this analysis demonstrates that the two tests are similar with

Figure 3.10: Mouse cylinder test paw-dragging behaviour.

A-D) Representative photographs of a mouse performing a cylinder rear without forelimb motor deficits. Photos are taken in succession from a video recording.

E-H) Representative photographs of a mouse performing a paw-drag. Photos are taken in succession from a video recording. Black arrows indicate the affected forepaw.
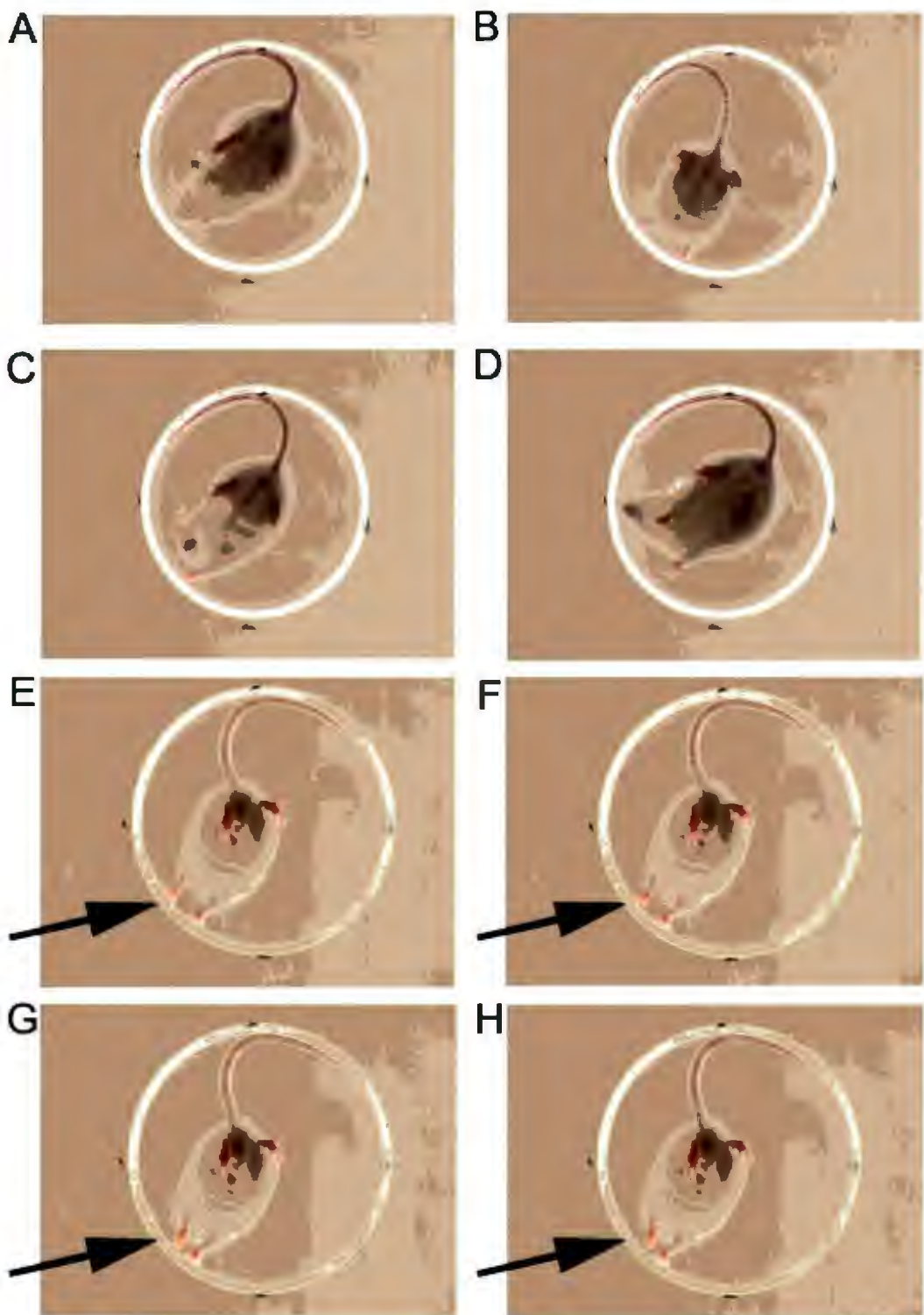
Figure 3.10

Figure 3.11: Paw-dragging analysis of the mouse cylinder test correlates with infarcts in the FMC.

A) Analysis of cylinder paw-dragging data for 2 cortical injections. (n=8 Saline, n=24 ET-1)

B) Analysis of cylinder paw-dragging data for 3 cortical injections. (n=13 Saline, n=16 ET-1)

C) Regression analysis of depth maps of the FMC_{60-100} at $\geq$60% cortical depth of infarcted tissue vs paw-dragging data for ET-1 injected mice at 3 days (R^2 0.195, p<0.01, slope=0.269), 1 week (R^2=0.066, p=0.115, slope=0.122) or at 2 weeks (R^2 0.182, p<0.01, slope=0.226). (n=39).

D) Regression analysis of depth maps of the FMC_{40-100} at >60% cortical depth of infarcted tissue vs paw-dragging data for ET-1 injected mice at 3 days (R^2=0.242, p<0.01, slope=0.393), 1 week (R^2=0.149, p<0.05, slope 0.240) or at 2 weeks (R^2 0.191, p<0.01, slope 0.293). (n 39).

E) Regression analysis of 1 week staircase deficits vs 3 day (R^2 0.076, p 0.122, slope 0.148) and 7 day (R^2=0.145, p<0.05, slope 0.126) paw-dragging for ET-1 injected mice. (n=34) *p<0.05, **p<0.01, ***p<0.001

Figure 3.11

respect to one another — something that should be expected if both tests seek the same relationship (increased core coverage with increased behavioural deficits). Despite these tests mildly relating to one another, the fact that they are both sensitive to FMC damage means that there is a greater chance that functional recovery can be observed when using both tests in a therapeutic experiment.

3.6 - Paw-dragging does not correlate with infarcts in either the anterior or posterior FMC alone.
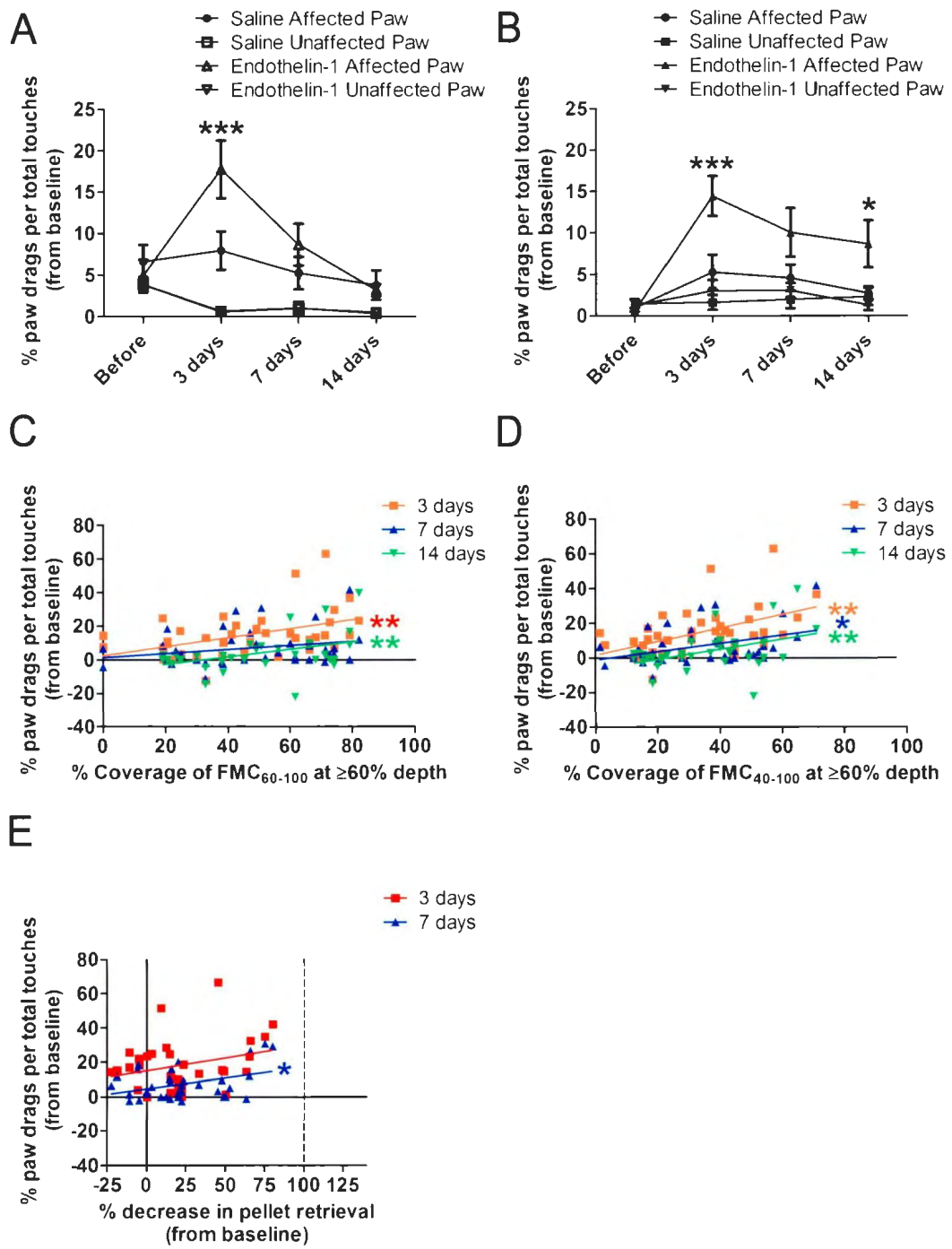
When comparing paw-dragging behaviour to coverage of the anterior FMC, there was no correlation. When comparing behaviour to core coverage in the FMC_{60-100} at >80% depth (Fig 3.12A), at >60% depth (Fig 3.12C) and of the FMC_{40-100} at >60% depth (Fig 3.12E) there were no correlations. There was a significant relationship at 14 days when comparing coverage of the posterior FMC_{60-100} at >80% depth (Fig 3.12B), $\geq60\%$ depth (Fig 3.12D) and the FMC_{40-100} at $\geq60\%$ depth (Fig 3.12F) to paw-dragging behaviour. These correlations, despite being significant, take place within a very narrow range of paw-dragging values — because of this, determining criteria based on these data may not be possible. While significant relationships emerge, the slope is quite low signifying that large injuries encompassing most of the FMC as a whole are conducive to paw-dragging behaviour.

3.7 — ET-1 infarcts in the FMC induce NPC proliferation and migration toward the ischemic cortex.

While ET-1 can produce behavioural deficits when targeted to the FMC, there are other considerations in developing an injury model. When considering therapy manipulating NPCs to regenerate infarcted neural tissue, it must be known whether NPCs endogenously repair small focal cerebral infarcts. While NPCs have been shown to migrate and differentiate into neurons after MCAO, the question must be asked again as ET-1 infarcts are smaller than those resulting from MCAO. Therefore, whether ET-1

78

Figure 3.12: Paw-dragging is not associated with ET-1 infarcts specifically in the anterior FMC.

A) Regression analysis of coverage of the anterior FMC_{60-100} at $\geq 80\%$ cortical depth of infarcted tissue vs paw-dragging data for ET-1 injected mice at 3 days ($R^2=0.014$, p=0.472, slope−0.065), 1 week (R^2 0.032, p−0.267, slope=0.071) or at 2 weeks ($R^2=0.003$, p 0.742, slope 0.021). (n 40)

B) Regression analysis of coverage of the posterior FMC_{60-100} at $>80\%$ cortical depth of infarcted tissue vs paw-dragging data for ET-1 injected mice at 3 days (R^2 0.046, p 0.183, slope 0.108), 1 week ($R^2=0.022$, p 0.361, slope=0.052) or at 2 weeks ($R^2=0.208$, p<0.01, slope=0.161). (n=40).

C) Regression analysis of coverage of the anterior FMC_{60-100} at $>60\%$ cortical depth of infarcted tissue vs paw-dragging data for ET-1 injected mice at 3 days ($R^2=0.091$, p−0.059, slope−0.159), 1 week (R^2 0.059, p 0.130, slope=0.090) or at 2 weeks (R^2 0.008, p 0.592, slope 0.032). (n 40)

D) Regression analysis of coverage of the posterior FMC_{60-100} at $\geq 60\%$ cortical depth of infarcted tissue vs paw-dragging data for ET-1 injected mice at 3 days (R^2 =0.073, p−0.092, slope 0.124), 1 week ($R^2=0.001$, p−0.819, slope 0.012) or at 2 weeks (R^2−0.192, p<0.01, slope 0.141). (n 40).

E) Regression analysis of coverage of the anterior FMC_{40-100} at $\geq 60\%$ cortical depth of infarcted tissue vs paw-dragging data for ET-1 injected mice at 3 days (R^2 −0.070, p−0.099, slope=0.174), 1 week ($R^2=0.076$, p 0.086, slope=0.127) or at 2 weeks (R^2 0.000, p 0.971, slope -0.003). (n=40)

F) Regression analysis of coverage of the posterior FMC_{40-100} at $\geq 60\%$ cortical depth of infarcted tissue vs paw-dragging data for ET-1 injected mice at 3 days ($R^2=0.090$, p−0.060, slope−0.173), 1 week (R^2 0.062, p−0.121, slope 0.101) or at 2 weeks (R^2 0.314, p<0.001, slope 0.226). (n 40) **p<0.01, ***p<0.001
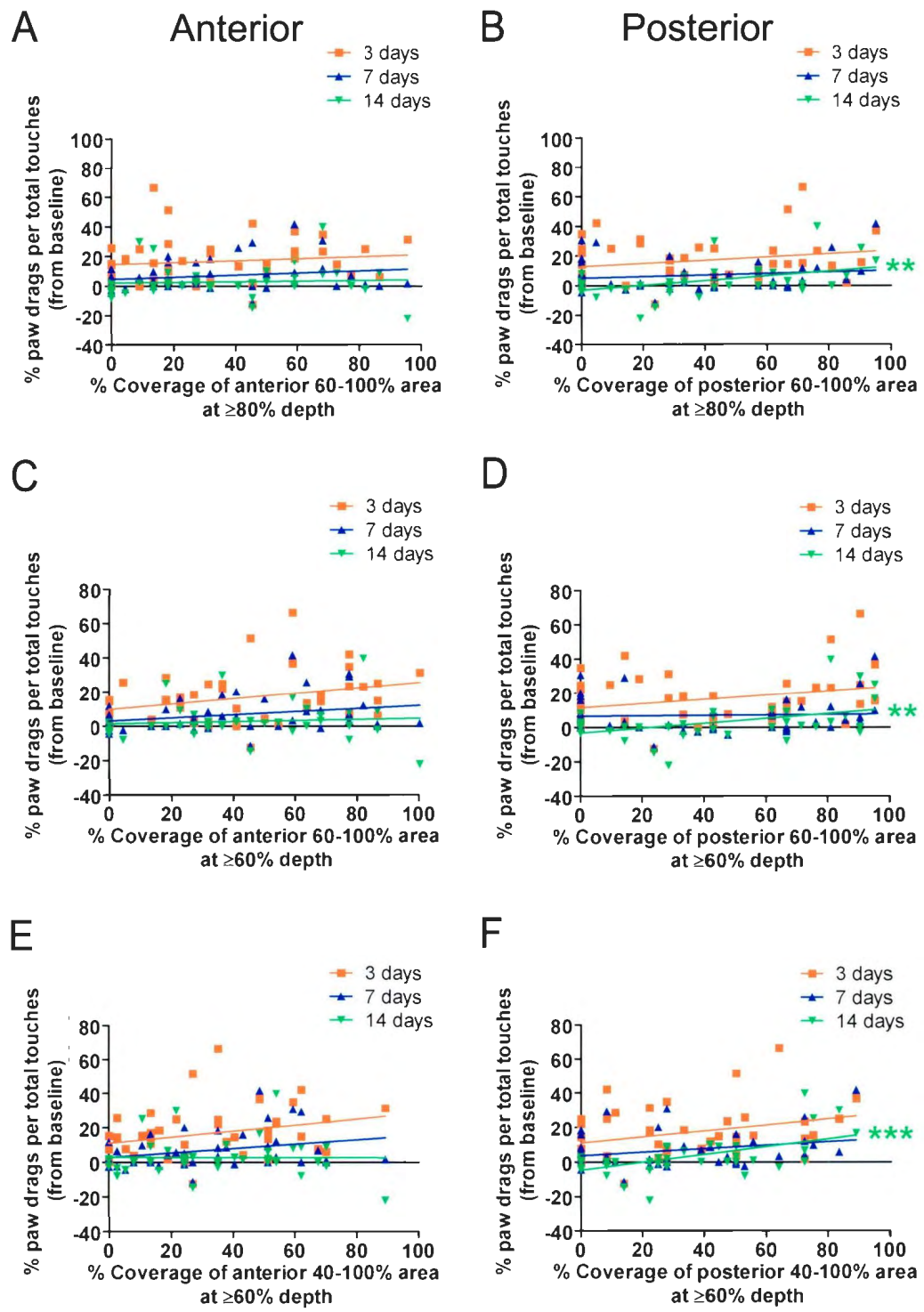
Figure 3.12

infarcts in the FMC promote NPC proliferation and migration toward the ischemic cortex was assessed. To study this, daily BrdU injections were given on post-surgery days 4-8, labeling NPC's undergoing terminal mitosis. By observing Dex+/BrdU+ cells outside of the SVZ, NPC migration can be quantified. Dex+ BrdU+ double-labeled cells were shown migrating from the SVZ toward the infarct, demonstrating that Dex+ neuroblasts born on days 4-8 post-injection leave the SVZ and migrate toward ischemic injury (Fig 3.13A). Proliferation can be assessed by analyzing the number of Dex+ neuroblasts in the ipsilateral SVZ as opposed to the contralateral SVZ. While this assay does not measure the number of proliferating cells, it measures an increase in the number of Dex+ neuroblasts generated which likely result from increased NPC proliferation. The diagram in Fig 3.13B encloses the lateral ventricle and SVZ, outside which neuroblasts are said to be migrating toward the injured tissue. An increase in the number of Dex+ cells in the SVZ was observed ipsilateral to the injury, compared to the contralateral SVZ, suggesting that increased NPC proliferation has occurred and/or is occurring in response to ischemic injury (Fig 3.13C). While Dex+ cell numbers are increased in the cortex ipsilateral to the injury, migration of Dex+ cells away from the SVZ was compared to that in the contralateral cortex. There were a significant number of Dex+ neuroblasts migrating toward the injury at 0-150μm from the SVZ (Fig 3.13D). Neuroblasts are found further than 150μm from the SVZ, but their numbers were variable, suggesting that they either die or differentiate into Dex- neurons. Together, these results suggest that a significant number of neuroblasts migrate toward the injured cortex and corpus callosum.

Figure 3.13 Neural precursor cells proliferate and migrate toward an ET-1 induced cortical ischemic injury.

A) Immunohistochemistry for Dcx+(green) and BrdU+(red) cells in the injured hemisphere.

B) Right cerebral hemisphere depicting SVZ in red boxed area. Cells found outside this area were counted as migrating (adapted from Doetsch et al., 1999).

C) Comparing the number of Dcx+ cells in the SVZ between injured and uninjured hemispheres (n=7).

D) Comparing the number of Dcx+ cells migrating away from the SVZ in 150μm increments from the SVZ in injured and uninjured hemispheres (n=7).

$F_{distance}(3,72)=3.56$. *p<0.05

A

Doublecortin 20x

BrdU 20x

Merge 20x

50 μm

Merge 10x

Cortex

Corpus Callosum

SVZ

200 μm

B

LV

C

□ Uninjured Side
■ Injured Side

Number of Dcx+ cells

2000

1500

1000

500

0

*

Ventricle

D

Number of Dcx+ cells

150

100

50

0

*

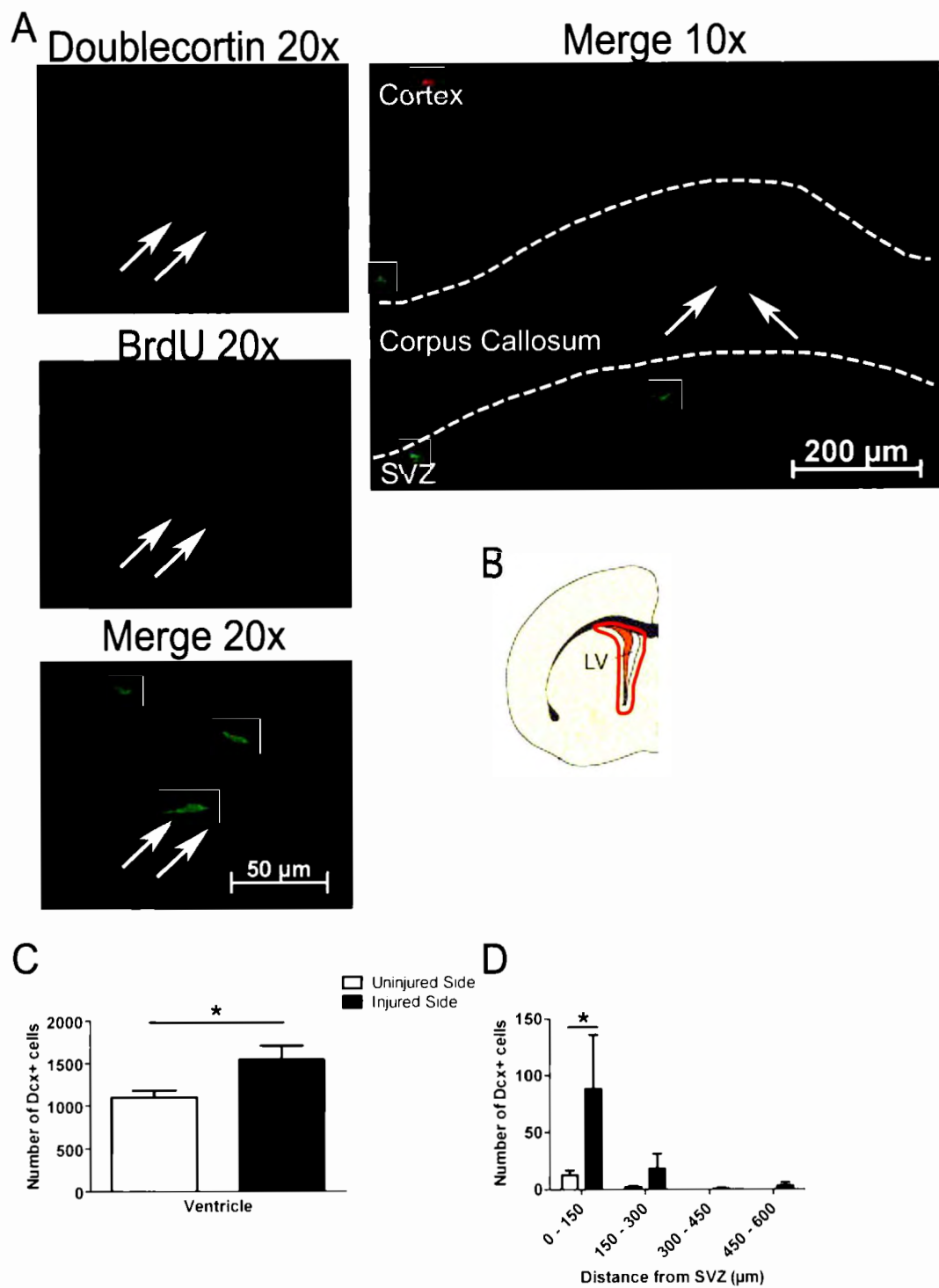0 - 150   150 - 300   300 - 450   450 - 600

Distance from SVZ (μm)

Figure 3.13

Chapter 4: Discussion

In this study it was shown that a reproducible ET-1 induced ischemic injury can be produced in the mouse cerebral cortex which correlates with behavioural deficits. The mouse staircase test was shown to correlate with location and depth of an ET-1 induced ischemic injury in the mouse FMC. The FMC was also shown to be functionally subdivided: damage in the anterior FMC is highly correlated with deficits in the mouse staircase while damage in the posterior FMC is not. This study confirms previous studies showing that analysis of percentage of affected paw use in the cylinder test of forelimb asymmetry does not correlate with ET-1 injury in the FMC. However, I developed a novel analysis of the mouse cylinder test, "paw-dragging", which does correlate with an ET-1 induced ischemic injury to the FMC. Additionally, ET-1 induced ischemic injury is associated with greater numbers of SVZ NPCs and their migrative response. An increase in the number of Doublecortin+ NPCs in the ipsilateral SVZ and corpus callosum was observed two weeks after an ET-1 induced ischemic injury, demonstrating that NPCs are migrating toward the injury site. These findings demonstrate that a focal ischemic injury in the mouse FMC correlates with behavioural tests, and that SVZ NPCs migrate toward the injured cortex.

4.1   A model of ET-1 induced ischemic injury has been produced in the mouse

In assessing NPC mediated regeneration of cortical tissue in the mouse, an injury model must be developed such that the injury is consistently associated with behavioural deficits but small enough to be repaired. Due to this, creating an injury model using focal ET-1 induced ischemic injuries would be most appropriate in assessing NPC mediated regeneration of cortical tissue. Other types of injury, such as MCAO induced ischemia, produce much larger injuries encompassing much of the striatum and lateral cerebral cortex (Tamura et al., 1981) and may prove more difficult to regenerate lost neural tissue. While ET-1 is a potent vasoconstrictor, a potential drawback to using exogenous ET-1 is that it relies on pharmacological intervention, creating levels of ET-1 which would never

ordinarily occur *in vivo*. ET-1 affects other cell types due to the ET-B receptor being present in NPC's and cortical astrocytes this can cause the release of factors affecting vascular permeability and astrocyte proliferation (Koyama et al., 2012; Nishikawa et al., 2011). However, the controllable size and ability to target the injury to a specific location allows it to answer questions that may be more challenging to address using MCAO, such as whether therapies involving NPCs can improve functional recovery.

Consistent with the demands of the model, ET-1 produces a small but significant infarct size and these experiments show that it produces measurable behavioural deficits on the staircase and mouse cylinder tests. The concentration of ET-1 used here ($2\mu g/\mu l$) was higher than that used in other studies of ET-1 injections in the mouse cortex, though injections made herein using the lower concentration of ET-1 ($1\mu g/\mu l$) were difficult to resolve and did not seem to produce a reliable behavioural deficit (Wang et al., 2007b, Tennant et al., 2009, Sozmen et al., 2009). The infarct size is dependent on the number of injections, demonstrating that the size of injuries are controllable and that cortical regions of interest can be damaged while sparing other regions. The ability to specify the size and location of the injury make ET-1 induced ischemia a more desirable model than others when assessing regeneration of cortical tissue in mice.

4.2 - Mouse staircase behaviour correlates with the location of ET-1 infarcts

This study is the first to demonstrate that the mouse staircase test correlates with FMC damage after ET-1 induced ischemic injury. While the mouse staircase test is effective in predicting MCAO induced ischemic injury and cortical aspiration lesions, it was unclear whether a smaller focal injury could reliably induce significant deficits (Baird et al., 2001, Bouët et al., 2007). The staircase test is effective in predicting MCAO and ET-1 induced ischemic injuries in rats as well; however, this may be due to the fact that ET-1 produces larger infarcts in rats than in mice, encompassing a wider brain volume and damaging multiple functional circuits (Windle et al., 2006). These experiments demonstrate that precise targeting of ET-1 to forelimb representations in the mouse motor cortex produces a significant behavioural deficit, despite the fact that ET-1

induced infarcts are much smaller than MCAO induced infarcts.

The mouse staircase test specifically correlates with injury in the anterior FMC. This is consistent with recent findings that abduction of the mouse forelimb is a result of activity in the anterior FMC while adduction of the forelimb is a result of activity in the posterior FMC (Harrison et al., 2012). It is difficult to directly compare staircase reaching with forelimb abduction because forelimb reaching involves a series of movements and several muscle groups. However, both movements share an anterior movement of the forelimb, suggesting that a common representation may exist in the FMC. These results supply additional information on the mouse FMC map developed by Tennant & colleagues as well as the mouse motor cortex region by Franklin & Paxinos (Franklin & Paxinos., 2004, Tennant et al., 2011). Additionally, by examining only mice which have anterior FMC damage, I have shown that these animals have significantly larger staircase deficits than ET-1 injected animals with damage outside the anterior FMC ("OFF-target" injuries). While there is no significant difference between saline-injected animals and ON-target ET-1 injected animals at 2 weeks, this is largely because there is more variability in groups once they have been split into their ON and OFF-target groups, respectively. Increasing the number of mice in this analysis would be a large undertaking, but it would be expected that ET-1 ON-target injections would have significantly larger staircase deficits than other groups. Demonstrating the regional functionality in the FMC holds promise not only in understanding the organization of the mouse motor cortex, but also in developing and refining models of cortical injury.

4.3 - Paw-dragging behaviour correlates with the location of ET-1 infarcts

In addition to the staircase test, paw-dragging analysis of the mouse cylinder test correlates highly with FMC injury. Paw-dragging analysis is useful in that it is more sensitive to FMC damage than forelimb asymmetry analysis, which showed no deficits in this study after ET-1 injection. While forelimb asymmetry deficits are apparent after larger infarcts such as MCAO, smaller infarcts such as ET-1 induced cortical injury do not show deficits in forelimb asymmetry (Tennant et al., 2009). This reinforces the idea

that the size of infarct as well as location may be a major determinant of deficit. Paw-dragging may have a niche use in smaller injuries where forelimb asymmetry is not useful (as opposed to larger injuries where forelimb asymmetry deficits correlate with damage).

Paw-dragging deficits tend to recover somewhat over time after either two or three injections of ET-1. However, paw-dragging behaviour is still significantly elevated at 14 days in the 3 injection group, while paw-dragging behaviour is only elevated after 3 days in the 2 injection group. This demonstrates that paw-dragging is sensitive to small changes in the amount of damage to the FMC, and greater damage produces more sustained deficits. The pattern of recovery of function after 2-injections is similar to studies showing that, post-MCAO, rats tend to have greater forelimb asymmetry deficits at 2 days post-MCAO then recover some function at 1 week post-MCAO (Encarnacion et al., 2011). Paw-dragging may also find use in other types of focal ischemic injury models such as those induced by photothrombosis. Further study is required to determine how inclusionary criteria can be developed from this highly sensitive test of forelimb motor deficit.

Paw-dragging has been shown here to correlate positively, albeit weakly, with staircase retrieval. As paw-dragging does not seem to arise specifically from anterior FMC damage, it is likely that paw-dragging and staircase deficits arise from damage to different subdivisions of the FMC. As both tests are responsive to FMC damage, this allows for each test to potentially respond to damage that the other wouldn't, increasing the chances that an infarct has a behavioural correlate. It is possible that paw-dragging results from damage to the forelimb sensorimotor cortex, though this has not been examined in this study. The fact that paw-dragging is observed at some level in every mouse given an FMC injection of ET-1 suggests otherwise, though more investigation is needed.

4.4   NPC proliferation and migration in response to ET-1 infarcts

NPC proliferation after ET-1 induced ischemic injury has previously been

demonstrated in mice 3 days post-ischemia (Wang et al., 2007b). While my experiments demonstrate increased Dex+ cells in the SVZ at 14d post-ischemia, both studies demonstrate increased Dex+ SVZ neuroblasts following cortical ET-1 injections. This lends support to the theory that cortical ischemia can induce proliferation, though a true proliferation assay must be performed. Having an increased pool of neuroblasts which migrate toward the infarct and regenerate lost tissue is an advantage when using stroke therapies focused on fortifying SVZ neuroblasts with pro-survival factors.

While NPCs are known to proliferate and migrate toward a large CNS injury such as MCAO, this study demonstrates that a focal ET-1 induced cortical ischemic injury is associated with neuroblast migration in the mouse. The volume of migrating neuroblasts peaks between 7 and 14 days post-MCAO in the rat (Arvidsson et al., 2002). While the peak volume of migration has not been assessed with smaller ET-1 injuries in mice, my results show that there is still a measurable response at 14 days post-ischemia. A significant increase in the number of neuroblasts in the corpus callosum of the injured hemisphere was observed when assessing only neuroblasts within 150μm from the edge of the SVZ. Furthermore, there are fewer neuroblasts and more variability in their numbers as the distance from the SVZ increases. This may be due to a number of reasons, including neuroblasts moving into the cortex where there may be an increased probability of apoptosis. Furthermore, some neuroblasts may have already differentiated into mature neurons, in which case Dex would no longer be expressed. As neuroblasts migrate closer to the injured cortex, both of these possibilities would seem more likely. Despite some uncertainty as to their fate, the migration of NPCs into the damaged cortex is evident, allowing future studies to develop therapies targeting and modifying NPCs.

4.5   Summary

In summary, it has been shown that ET-1 produces a reproducible focal ischemic cortical injury in the mouse FMC. This study is the first to link increasing damage to the FMC to deficits in the staircase test. Moreover, this study demonstrates that the staircase test correlates with anterior FMC damage rather than posterior FMC damage   a

phenomenon which may be explained by recent work examining subdivisions of the mouse FMC (Harrison et al., 2012). A new assessment of the mouse cylinder test - paw-dragging   has been developed which correlates with ET-1 induced ischemic injury in the FMC. This test is highly sensitive to injury within the mouse FMC and, with further study, can be used as an early measurement tool to exclude uninjured mice from future regeneration studies. Finally, for future studies investigating NPC mediated regeneration of cortical tissue, it has been shown that ET-1 induced ischemic injury elicits an endogenous neurogenic response in the mouse cortex. An increased number of Dcx+ neuroblasts in the SVZ of injured mice were observed. As well, NPC migration toward an ET-1 induced focal ischemic injury has been observed in the mouse for the first time. These findings will allow investigators to use a wide variety of transgenic mice to investigate therapies for cortical ischemia. This work will allow significant strides to be made in mouse regenerative medicine and, from this, a hurdle toward developing new therapies is removed.

4.6   Future directions

While this model of ischemic injury includes quantifiable deficits on the mouse staircase test and cylinder test, there are some considerations that must be met before it can be used to study regenerative therapies using NPCs.

The first consideration is that the model only observes deficits up to 14 days post-injection. Future work will need to observe long term deficits in order to model long term deficits in humans after ischemic stroke. This experiment will involve three injections of ET-1, but will continue to test mice on both behavioural tests up to 28 days post-injection. Staircase and cylinder testing will occur every week including 21 and 28 days post-injection. By developing a long-lasting behavioural deficit, one can assess recovery of function with different regenerative therapies.

The second consideration is that during this experiment, the anterior FMC was identified as being responsible for motor movements crucial for staircase pellet retrieval. This region is slightly anterior to the target of the current injection sites: the 80-100%

FMC core. Deficits in this test should be made more pronounced, as the effect size is significant but small. Future experiments will need to modify the injection sites such that the anterior FMC can be maximally damaged. As infarcts covering the majority of the anterior FMC produce modest deficits on the staircase test, adjusting the injection sites to maximize infarct coverage will be crucial in order to observe functional recovery afterward. This could be achieved by adding additional injections of ET-1 or by increasing the spacing between injections to create a broader injury encompassing most of the anterior FMC. By consistently damaging the anterior FMC, it may be possible to produce more pronounced behavioural deficits more frequently and reduce inter-animal variability. Beyond refinement of the injury model however, regenerative therapies must be developed.

After an injury model is refined, therapies promoting neural regeneration can take advantage of it. There are some issues with the endogenous neurogenic response to injury that may need to be dealt with before an effective therapy is produced.

It has already been demonstrated that NPCs can migrate toward a site of injury and differentiate into locally relevant subtypes: namely, SVZ neuroblasts differentiating into DARPP32+ medium spiny neurons which are specific to the striatum (Arvidsson et al., 2002). Critics of this view may note that medium spiny neurons in the striatum are still GABAergic, and are more similar to the NPCs which normally give rise to GABAergic granule cells in the olfactory bulb (Whitman & Greer, 2009). However, NPCs in the dorsal horn of the SVZ display a phenotype consistent with early glutamatergic cortical precursors and can differentiate into glutamatergic neurons *in vitro* (Brill et al., 2009). This suggests that two factors can affect the subtype of an adult born neuron: cues local to the region that it migrates into, and cues within the SVZ which promote subtype specification. How these two factors interact to produce specific neuronal subtypes after ischemic stroke is not yet clear. Recently, Shh release from neurons in the ventral septum was shown to affect NPC subtype specification in the adult SVZ (Ihrie et al., 2011). Despite subtype specification being a valid concern for a model of neural regeneration, this evidence suggests that cells may differentiate into relevant subtypes without the need for external intervention. Integration into the appropriate

neural circuits, however, is another concern. While interneurons may have less difficulty forming new synapses, neurons in layers normally projecting subcortically or interhemispherally may not be able to recapitulate axon guidance that occurs during development. Whether this is possible or not is not yet known.

Aside from issues regarding subtype specification, other issues arise when trying to fortify NPCs using gene therapy. In order to test whether Mcl-1 can improve survival of migrating NPCs, further study must identify peak NPC migration times as well as the most efficient route of NPC transfection or infection. Two routes which hold promise for delivery of pro-survival factors such as Mcl-1 are adult electroporation and retroviral infection (Barnabé-Heider et al., 2008; Goings et al., 2004). Assessing rates of transduction will be key in determining which method is optimum. As well, since Mcl-1 promotes cell cycle exit in NPCs, expressing Mcl-1 from a Dcx promoter in neuroblasts may prevent Mcl-1 from causing B and C cells to prematurely differentiate, allowing expansion of the NPC population (Hasan et al., in press, Wang et al., 2007a). While creation of a transgenic Dcx-Mcl-1 mouse may be the most efficient way of ensuring Mcl-1 is expressed in neuroblasts, there is significant cost overhead in producing and maintaining transgenic mouse strains.

Regenerative therapies continue to be developed and refined in animal models. Of these therapeutic studies, many show degrees of functional recovery within subjects. Some studies show that while NPC migration and/or grafts integrate somewhat with local circuits they provide trophic support for damaged cells by emitting growth factors (Doeppner et al., 2010). While modifying endogenous NPCs is an attractive avenue for therapy, NPC grafts may be a more attractive human therapy as NPCs can be injected at the site of interest and genetic modifications can be performed prior to surgery. Whether NPCs integrate into circuits or simply provide trophic support to injured cells in the peri-infarct cortex will need to be determined. The consensus favours therapeutic interventions using NPCs rather than not using NPCs when aiming for functional recovery. By improving the survival of NPCs, they may integrate into local circuits or simply provide trophic support over a longer period of time. Potentially, Mcl-1 has the ability to improve prognosis post-stroke via either process.

91

Despite a number of challenges, the case for neural regeneration remains strong. From this work, the model should continue to be refined until the set of injection sites allow for an ischemic injury covering the relevant cortical areas while minimalizing damage to unrelated cortical areas. Furthermore, the injury model must be validated in the long-term such that the benefits can be detected from the prolonged generation of adult born neurons. Challenges such as gene transduction efficiencies and peak migration times must be identified and taken advantage of, but are realistic goals. As well, the challenge of subtype specification may even be moot, as the fate of NPCs is reasonably plastic post-stroke, and there is even a diversity of subtypes within the SVZ. Despite there being challenges in developing neural regeneration therapies, the evidence is encouraging that neural regeneration matters, and it is quite clear that these challenges must be met in order to maximize success.

This work is currently being prepared for publication.

References:

Adachi, K., Mirzadeh, Z., Sakaguchi, M., Yamashita, T., Nikolcheva, T., Gotoh, Y., Peltz, G (2007). Beta-catenin signaling promotes proliferation of progenitor cells in the adult mouse subventricular zone. *Stem Cells, 25*(11), 2827-36.

Altman, J. (1962). Are new neurons formed in the brains of adult mammals? *Science, 135*(3509), 1127-1128.

Altman, J, & Das, G. D. (1965). Autoradiographic and Histoloaical Evidence of Postnatal Hippocampal Neurogenesis in Rats. *Journal of Comparative Neurology, 124*, 319-336.

Altman, J. & Das, G. D. (1969). Autoradiographic and Histological Studies of Postnatal Neurogenesis. IV. Cell proliferation and migration in the anterior forebrain, with special reference to persisting neurogenesis in the olfactory bulb. *Journal of Comparative Neurology, 137*(4), 433-457.

Altman, J. (1963). Autoradiographic Investigation of Cell Proliferation in the Brains of Rats and Cats. *The Anatomical Record, 145*, 573-591.

Altman, J. & Das, G. D. (1966). Autoradiographic and Histological Studies of Postnatal Neurogenesis. I. A LONGITUDINAL INVESTIGATION OF THE KINETICS, MIGRATION AND TRANSFORMATION OF CELLS INCORPORATING TRITIATED THYMIDINE IN NEONATE RATS, WITH SPECIAL REFERENCE TO POSTNATAL NEUROGENESIS. *Journal of Comparative Neurology, 126*(3), 337-390.

Arbour, N., Vanderluit, J. L., Le Grand, J. N., Jahani-Asl, A., Ruzhynsky, V. a, Cheung, E. C. C., Kelly, M. a, et al. (2008). Mcl-1 is a key regulator of apoptosis during CNS development and after DNA damage. *The Journal of Neuroscience, 28*(24), 6068-78.

Arvidsson, A., Collin, T., Kirik, D., Kokaia, Z., & Lindvall, O. (2002). Neuronal replacement from endogenous precursors in the adult brain after stroke. *Nature Medicine, 8*(9), 963-70.

Astrup, J., Siesjo, B. K., & Symon, L. (1981). Thresholds in cerebral ischemia - the ischemic penumbra. *Stroke, 12*(6), 723-725.

Astrup, J., Symon, L., Branston, N. M., & Lassen, N. a. (1977). Cortical evoked potential and extracellular K+ and H+ at critical levels of brain ischemia. *Stroke, 8*(1), 51-57.

Baird, a L., Meldrum, a, & Dunnett, S. B. (2001). The staircase test of skilled reaching in mice. *Brain Research Bulletin, 54*(2), 243-50.

Barnabe-Heider, F., Meletis, K., Eriksson, M., Bergmann, O., Sabelstrom, H., Harvey, M. A., et al. (2008). Genetic manipulation of adult mouse neurogenic niches by in vivo electroporation. *Nature Methods, 5*(2), 189-196.

Baskin, Y. K., Dietrich, W. D., & Green, E. J. (2003). Two effective behavioral tasks for evaluating sensorimotor dysfunction following traumatic brain injury in mice. *Journal of Neuroscience Methods, 129*(1), 87-93.

Bouët, V., Freret, T., Toutain, J., Divoux, D., Boulouard, M., & Schumann-Bard, P. (2007). Sensorimotor and cognitive deficits after transient middle cerebral artery occlusion in the mouse. *Experimental Neurology, 203*(2), 555-67.

Brill, M. S., Ninkovic, J., Winpenny, E., Hodge, R. D., Ozen, I., Yang, R., Lepier, A., et al. (2009). Adult generation of glutamatergic olfactory bulb interneurons. *Nature Neuroscience, 12*(12), 1524-33.

Chiasson, B. J., Tropepe, V., Morshead, C. M., & Kooy, D. V. D. (1999). Adult Mammalian Forebrain Ependymal and Subependymal Cells Demonstrate Proliferative Potential, but only Subependymal Cells Have Neural Stem Cell Characteristics. *The Journal of Neuroscience, 19*(11), 4462-4471.

Chipuk, J. E., Moldoveanu, T., Llambi, F., Parsons, M. J., & Green, D. R. (2010). The BCL-2 family reunion. *Molecular Cell, 37*(3), 299-310.

Craig, C.G, Morshead, C.M., Roach, A., & van der Kooy, D. (1994). Evidence for a relatively quiescent stem cell in the adult mammalian forebrain. *Journal of Cellular Biochemistry, 18* (Suppl.), 176.

Craig, C.G., Tropepe, V., Reynolds, A., & Tn, C. (1996). In Viva Growth Factor Expansion Neural Precursor Cell Populations of Endogenous Subependymal in the Adult Mouse Brain. *Journal of Comparative Neurology, 16*(8), 2649-2658.

Davenport, A. P. (2002). International Union of Pharmacology. XXIX. Update on endothelin receptor nomenclature. *Pharmacological Reviews, 54*(2), 219-26.

Derbyshire, E. R., & Marletta, M. A. (2009). Biochemistry of Soluble Guanylate Cyclase. *Handbook of Experimental Pharmacology, 191*, 17-31.

Dirnagl, U., Iadecola, C., & Moskowitz, M. a. (1999). Pathobiology of ischaemic stroke: an integrated view. *Trends in Neurosciences, 22*(9), 391-7.

Doeppner, T. R., Dietz, G. P. H., El Aanbouri, M., Gerber, J., Witte, O. W., Bähr, M., & Weise, J. (2009). TAT-Bcl-x(L) improves survival of neuronal precursor cells in the lesioned striatum after focal cerebral ischemia. *Neurobiology of Disease, 34*(1), 87-94.

Doeppner, T. R., El Aanbouri, M., Dietz, G. P. H., Weise, J., Schwarting, S., & Bähr, M. (2010). Transplantation of TAT-Bcl-xL-transduced neural precursor cells: long-term neuroprotection after stroke. *Neurobiology of Disease, 40*(1), 265-76.

Doetsch, F., & Alvarez-Buylla, a. (1996). Network of tangential pathways for neuronal migration in adult mammalian brain. *Proceedings of the National Academy of Sciences of the United States of America, 93*(25), 14895-900.

Doetsch, F., Caillé, I., Lim, D. a, García-Verdugo, J. M., & Alvarez-Buylla, A. (1999). Subventricular zone astrocytes are neural stem cells in the adult mammalian brain. *Cell, 97*(6), 703-16.

Doetsch, F., Garcia-Verdugo, J. M., & Alvarez-Buylla, a. (1999). Regeneration of a germinal layer in the adult mammalian brain. *Proceedings of the National Academy of Sciences of the United States of America, 96*(20), 11619-24.

Doetsch, F., García-Verdugo, J. M., & Alvarez-Buylla, A. (1997). Cellular composition and three-dimensional organization of the subventricular germinal zone in the adult

mammalian brain. *The Journal of Neuroscience, 17*(13), 5046-61.

Encarnacion, A., Horie, N., Keren-Gill, H., Bliss, T. M., Steinberg, G. K., & Shamloo, M. (2011). Long-term behavioral assessment of function in an experimental model for ischemic stroke. *Journal of Neuroscience Methods, 196*(2), 247-57.

Engel, O., Kolodziej, S., Dirnagl, U., & Prinz, V. (2011). Modeling Stroke in Mice - Middle Cerebral Artery Occlusion with the Filament Model. *Journal of Visualized Experiments, 47*, 2423.

Farr, T. D., Liu, L., Colwell, K. L., Whishaw, I. Q., & Metz, G. A. (2006). Bilateral alteration in stepping pattern after unilateral motor cortex injury : A new test strategy for analysis of skilled limb movements in neurological mouse models. *Journal of Neuroscience Methods, 153*, 104-113.

Franklin, K. B. J., & Paxinos, G. (2004). *The Mouse Brain in Stereotaxic Coordinates.* J. Menzel (Ed.). Academic Press, New York, NY.

Fuxe, N., Kurosawa, N., Cintra, A., Hallstrom, A., Goiny, M., Rosén, M., Agnati, L. ., et al. (1992). Involvement of local ischemia in endothelin-1 induced lesions of the neostriatum of the anaesthetized rat. *Experimental Brain Research, 88*, 131-139.

Goings, G. E., Sahni, V., & Szele, F. G. (2004). Migration patterns of subventricular zone cells in adult mice change after cerebral cortex injury. *Brain Research, 996*, 213 - 226.

Gordon, R. J., Tattersfield, a S., Vazey, E. M., Kells, a P., McGregor, a L., Hughes, S. M., & Connor, B. (2007). Temporal profile of subventricular zone progenitor cell migration following quinolinic acid-induced striatal cell loss. *Neuroscience, 146*(4), 1704-18.

Gritti, a, Cova, L., Parati, E. a, Galli, R., & Vescovi, a L. (1995). Basic fibroblast growth factor supports the proliferation of epidermal growth factor-generated neuronal precursor cells of the adult mouse CNS. *Neuroscience Letters, 185*(3), 151-4.

Gu, W., Brännström, T., & Wester, P. (2000). Cortical neurogenesis in adult rats after

reversible photothrombotic stroke. *Journal of Cerebral Blood Flow and Metabolism,* *20*(8), 1166-73.

Harrison, T. C., Ayling, O. G. S., & Murphy, T. H. (2012). Distinct cortical circuit mechanisms for complex forelimb movement and motor map topography. *Neuron,* *74*(2), 397-409.

Hasan, S.M.M., Sheen, A.D, Power, A.M, Langevin, L.M, Xiong, J., Furlong, M., Day, K., Schuurmans, C., Opferman, J.T., Vanderluit, J.T. (in press at Development). Mcl-1 regulates terminal mitosis of neural precursor cells in the mammalian brain through p27^{kip1}.

Horie, N., Maag, A.-L., Hamilton, S. a, Shichinohe, H., Bliss, T. M., & Steinberg, G. K. (2008). Mouse model of focal cerebral ischemia using endothelin-1. *Journal of Neuroscience Methods,* *173*(2), 286-90.

Ihrie, R. a, Shah, J. K., Harwell, C. C., Levine, J. H., Guinto, C. D., Lezameta, M., Kriegstein, A. R., et al. (2011). Persistent sonic hedgehog signaling in adult brain determines neural stem cell positional identity. *Neuron,* *71*(2), 250-62.

Imayoshi, I., Sakamoto, M., Yamaguchi, M., Mori, K., & Kageyama, R. (2010). Essential roles of Notch signaling in maintenance of neural stem cells in developing and adult brains. *The Journal of Neuroscience,* *30*(9), 3489-98.

Jiang, W., Gu, W., Brännström, T., Rosqvist, R., & Wester, P. (2001). Cortical neurogenesis in adult rats after transient middle cerebral artery occlusion. *Stroke,* *32*(5), 1201-7.

Jin, K., Minami, M., Lan, J. Q., Mao, X. O., Batteur, S., Simon, R. P., & Greenberg, D. a. (2001). Neurogenesis in dentate subgranular zone and rostral subventricular zone after focal cerebral ischemia in the rat. *Proceedings of the National Academy of Sciences of the United States of America,* *98*(8), 4710-5.

Jin, Kunlin, Zhu, Y., Sun, Y., Mao, X. O., Xie, L., & Greenberg, D. a. (2002). Vascular endothelial growth factor (VEGF) stimulates neurogenesis in vitro and in vivo.

Proceedings of the National Academy of Sciences of the United States of America, 99(18), 11946-50.

Kilic, E., Dietz, G. P. H., Hermann, D. M., & Bähr, M. (2002). Intravenous TAT-Bcl-Xl is protective after middle cerebral artery occlusion in mice. *Annals of Neurology*, 52(5), 617-22.

Koyama, Y., Maebara, Y., Hayashi, M., Nagae, R., Tokuyama, S., & Michinaga, S. (2012). Endothelins reciprocally regulate VEGF-A and angiopoietin-1 production in cultured rat astrocytes: implications on astrocytic proliferation. *Glia*, 60(12), 1954-63.

Kozopas, K. M., Yang, T., Buchan, H. L., Zhou, P., & Craig, R. W. (1993). MCL1, a gene expressed in programmed myeloid cell differentiation, has sequence similarity to BCL2. *Proceedings of the National Academy of Sciences of the United States of America*, 90(8), 3516-20.

Kreuzberg, M., Kanov, E., Timofeev, O., Schwaninger, M., Monyer, H., & Khodosevich, K. (2010). Increased subventricular zone-derived cortical neurogenesis after ischemic lesion. *Experimental Neurology*, 226(1), 90-99.

Kuhn, H. G., Winkler, J., Kempermann, G., Thal, L. J., & Gage, F. H. (1997). Epidermal growth factor and fibroblast growth factor-2 have different effects on neural progenitors in the adult rat brain. *The Journal of Neuroscience*, 17(15), 5820-9.

Lehtinen, M. K., Zappaterra, M. W., Chen, X., Yang, Y. J., Hill, A. D., Lun, M., Maynard, T., et al. (2011). The cerebrospinal fluid provides a proliferative niche for neural progenitor cells. *Neuron*, 69(5), 893-905.

Lipton, P. (1999). Ischemic cell death in brain neurons. *Physiological Reviews*, 79(4), 1431-568.

Liu, C. L., Siesjö, B. K., & Hu, B. R. (2004). Pathogenesis of hippocampal neuronal death after hypoxia-ischemia changes during brain development. *Neuroscience*, 127(1), 113-23.

Liu, J., Solway, K., Messing, R. O., & Sharp, F. R. (1998). Increased neurogenesis in the dentate gyrus after transient global ischemia in gerbils. *The Journal of Neuroscience, 18*(19), 7768-78.

Lois, C., & Alvarez-Buylla, A. (1994). Long-distance neuronal migration in the adult mammalian brain. *Science, 264*(5162), 1145-8.

Lois, C., García-Verdugo, J. M., & Alvarez-Buylla, A. (1996). Chain migration of neuronal precursors. *Science, 271*(5251), 978-81.

Malone, C. D., Hasan, S. M. M., Roome, R. B., Xiong, J., Furlong, M., Opferman, J. T., & Vanderluit, J. L. (2012). Mcl-1 regulates the survival of adult neural precursor cells. *Molecular and Cellular Neurosciences, 49*(4), 439-47.

Michaelidis, T. M., Sendtner, M., Cooper, J. D., Airaksinen, M. S., Holtmann, B., Meyer, M., & Thoenen, H. (1996). Inactivation of bcl-2 results in progressive degeneration of motoneurons, sympathetic and sensory neurons during early postnatal development. *Neuron, 17*(1), 75-89.

Montoya, C. P., Campbell-Hope, L. J., Pemberton, K. D., & Dunnett, S. B. (1991). The "staircase test": a measure of independent forelimb reaching and grasping abilities in rats. *Journal of Neuroscience Methods, 36*(2-3), 219-28.

Morshead, C M. & van der Kooy, D. (1992). Postmitotic death is the fate of constitutively proliferating cells in the subependymal layer of the adult mouse brain. *The Journal of Neuroscience, 12*(1), 249-56.

Morshead, C M. Reynolds, B. a, Craig, C. G., McBurney, M. W., Staines, W. a, Morassutti, D., Weiss, S., et al. (1994). Neural stem cells in the adult mammalian forebrain: a relatively quiescent subpopulation of subependymal cells. *Neuron, 13*(5), 1071-82.

Morshead, C M., Garcia, a. D., Sofroniew, M. V., & van der Kooy, D. (2003). The ablation of glial fibrillary acidic protein-positive cells from the adult central nervous system results in the loss of forebrain neural stem cells but not retinal stem cells.

European Journal of Neuroscience, 18(1), 76-84.

Moskowitz, Michael a., Lo, E. H., & Iadecola, C. (2010). The science of stroke: mechanisms in search of treatments. *Neuron, 67*(2), 181-98. Elsevier Inc.

Nishikawa, K., Ayukawa, K., Hara, Y., Wada, K., & Aoki, S. (2011). Endothelin/endothelin-B receptor signals regulate ventricle-directed interkinetic nuclear migration of cerebral cortical neural progenitors. *Neurochemistry International, 58*(3), 261-72.

Ohab, J. J., Fleming, S., Blesch, A., & Carmichael, S. T. (2006). A neurovascular niche for neurogenesis after stroke. *The Journal of Neuroscience, 26*(50), 13007-16.

Okano, H., Sakaguchi, M., Ohki, K., Suzuki, N., & Sawamoto, K. (2007). Regeneration of the central nervous system using endogenous repair mechanisms. *Journal of Neurochemistry, 102*(5), 1459-65.

Palma, V., Lim, D. a, Dahmane, N., Sánchez, P., Brionne, T. C., Herzberg, C. D., Gitton, Y., et al. (2005). Sonic hedgehog controls stem cell behavior in the postnatal and adult brain. *Development, 132*(2), 335-44.

Parent, J. M., Vexler, Z. S., Gong, C., Derugin, N., & Ferriero, D. M. (2002). Rat forebrain neurogenesis and striatal neuron replacement after focal stroke. *Annals of Neurology, 52*(6), 802-13.

Reynolds, B. a, & Weiss, S. (1992). Generation of neurons and astrocytes from isolated cells of the adult mammalian central nervous system. *Science, 255*(5052), 1707-10.

Reynolds, B. a, & Weiss, S. (1996). Clonal and population analyses demonstrate that an EGF-responsive mammalian embryonic CNS precursor is a stem cell. *Developmental Biology, 175*(1), 1-13.

Rinkenberger, J. L., Horning, S., Klocke, B., Roth, K., & Korsmeyer, S. J. (2000). Mcl-1 deficiency results in peri-implantation embryonic lethality service Mcl-1 deficiency results in peri-implantation embryonic lethality. *Genes & Development, 14*(1), 23-27.

Roger, V. L., Go, A. S., Lloyd-Jones, D. M., Adams, R. J., Berry, J. D., Brown, T. M., Carnethon, M. R., et al. (2011). Heart disease and stroke statistics--2011 update: a report from the American Heart Association. *Circulation, 123*(4), e18-e209.

Rosamond, W., Flegal, K., Furie, K., Go, A., Haase, N., Hailpern, S. M., et al. (2008). Heart Disease and Stroke Statistics 2008 Update A Report From the American Heart Association Statistics Committee and Stroke Statistics Subcommittee. *Circulation, 117*(4), e25-e146.

Sacco, R. L., Benjaming, E. J., Broderick, J. P., Dyken, M., Easton, J. D., Feinberg, W. M., et al. (1997). Risk Factors. *Stroke, 28*, 1507-1517.

Sasaki, T., Kitagawa, K., Yagita, Y., Sugiura, S., Omura-matsuoka, E., Tanaka, S., et al. (2006). Bcl2 Enhances Survival of Newborn Neurons in the Normal and Ischemic Hippocampus. *Journal of Neuroscience Research, 1196*, 1187-1196.

Savitt, J. M., Jang, S. S., Mu, W., Dawson, V. L., & Dawson, T. M. (2005). Bcl-x is required for proper development of the mouse substantia nigra. *The Journal of Neuroscience, 25*(29), 6721-8.

Schallert, T., Fleming, S. M., Leasure, J. L., Tillerson, J. L., & Bland, S. T. (2000). CNS plasticity and assessment of forelimb sensorimotor outcome in unilateral rat models of stroke, cortical ablation, parkinsonism and spinal cord injury. *Neuropharmacology, 39*(5), 777-87.

Sozmen, E. G., Kolekar, A., Havton, L. a, & Carmichael, S. T. (2009). A white matter stroke model in the mouse: axonal damage, progenitor responses and MRI correlates. *Journal of Neuroscience Methods, 180*(2), 261-72.

Surks, H. K., & Surks, H. K. (2007). cGMP-Dependent Protein Kinase I and Smooth Muscle Relaxation A Tale of Two Isoforms. *Circulation Research, 101*, 1078-1080.

Saino, O., Taguchi, A., Nakagomi, T., Nakano-Doi, A., Kashiwamura, S.-I., Doe, N., Nakagomi, N., et al. (2010). Immunodeficiency reduces neural stem/progenitor cell apoptosis and enhances neurogenesis in the cerebral cortex after stroke. *Journal of*

Neuroscience Research, 88(11), 2385-97.

Statistics Canada. (2012). The Canadian Population in 2011: Age and Sex. Retrieved from http://www12.statcan.gc.ca/census-recensement/2011/as-sa/98-311-x/98-311-x2011001-eng.pdf.

Szele, F. G., & Chesselet, M.-francoise. (1996). Cortical Lesions Induce an Increase in Cell Number and PSA-NCAM Expression in the Subventricular Zone of Adult Rats. Journal of Comparative Neurology, 454, 439-454.

Tamura, A., Graham, D. I., McCulloch, J., & Teasdale, G. M. (1981). Focal cerebral ischaemia in the rat: 1. Description of technique and early neuropathological consequences following middle cerebral artery occlusion. Journal of Cerebral Blood Flow and Metabolism, 1(1), 53-60.

Taylor, R. C., Cullen, S. P., & Martin, S. J. (2008). Apoptosis: controlled demolition at the cellular level. Nature Reviews. Molecular Cell Biology, 9(3), 231-41.

Tennant, K. a, & Jones, T. a. (2009). Sensorimotor behavioral effects of endothelin-1 induced small cortical infarcts in C57BL/6 mice. Journal of Neuroscience Methods, 181(1), 18-26.

Tennant, K. a, Adkins, D. L., Donlan, N. a, Asay, A. L., Thomas, N., Kleim, J. a, & Jones, T. a. (2011). The organization of the forelimb representation of the C57BL/6 mouse motor cortex as defined by intracortical microstimulation and cytoarchitecture. Cerebral Cortex, 21(4), 865-76.

Tonchev, A. B., Yamashima, T., Sawamoto, K., & Okano, H. (2005). Enhanced proliferation of progenitor cells in the subventricular zone and limited neuronal production in the striatum and neocortex of adult macaque monkeys after global cerebral ischemia. Journal of Neuroscience Research, 81(6), 776-88.

Tonchev, A. B., Yamashima, T., Zhao, L., Okano, H. J., & Okano, H. (2003). Proliferation of neural and neuronal progenitors after global brain ischemia in young adult macaque monkeys. Molecular and Cellular Neuroscience, 23(2), 292-301.

Ulukaya, E., Acilan, C., & Yilmaz, Y. (2011). Apoptosis: why and how does it occur in biology? *Cell Biochemistry and Function, 29*(6) 468-480.

Vivien, D., Gauberti, M., Montagne, A., Defer, G., & Touzé, E. (2011). Impact of tissue plasminogen activator on the neurovascular unit: from clinical data to experimental evidence. *Journal of Cerebral Blood Flow and Metabolism, 31*(11), 2119-34.

Wang, X., Qiu, R., Tsark, W., and Lu, Q., (2007). Rapid promoter analysis in developing mouse brain and genetic labeling of young neurons by doublecortin-DsRed-express. *Journal of Neuroscience Research, 85*, 3567-3573.

Wang, Y, Jin, K., & Greenberg, D. a. (2007). Neurogenesis associated with endothelin-induced cortical infarction in the mouse. *Brain Research, 1167*, 118-22.

Watson, B. D., Dietrich, W. D., Busto, R., & Ginsberg, M. D. (1985). Induction of Reproducible Brain Infarction by Photochemically Initiated Thrombosis. *Annals of Neurology, 17*, 497-504.

Whitman, M. C., & Greer, C. a. (2009). Adult neurogenesis and the olfactory system. *Progress in Neurobiology, 89*(2), 162-75.

Wiley, K. E., & Davenport, A. P. (2004). Endothelin receptor pharmacology and function in the mouse: comparison with rat and man. *Journal of Cardiovascular Pharmacology, 44 Suppl 1*(December), S4-6.

Windle, V., Szymanska, A., Granter-Button, S., White, C., Buist, R., Peeling, J., & Corbett, D. (2006). An analysis of four different methods of producing focal cerebral ischemia with endothelin-1 in the rat. *Experimental Neurology, 201*(2), 324-34.

Youle, R. J., & Strasser, A. (2008). The BCL-2 protein family: opposing activities that mediate cell death. *Nature Reviews. Molecular Cell Biology, 9*(1), 47-59.

Yuan, J. (2009). Neuroprotective strategies targeting apoptotic and necrotic cell death for stroke. *Apoptosis, 14*(4), 469-477.

Zhang, R L., Zhang, Z. G., Zhang, L., & Chopp, M. (2001). Proliferation and differentiation of progenitor cells in the cortex and the subventricular zone in the

adult rat after focal cerebral ischemia. *Neuroscience*, *105*(1), 33-41.

Zhang, R L, Zhang, Z. G., Wang, Y., LeTourneau, Y., Liu, X. S., Zhang, X., Gregg, S. R.,
et al. (2007). Stroke induces ependymal cell transformation into radial glia in the
subventricular zone of the adult rodent brain. *Journal of Cerebral Blood Flow and
Metabolism*, *27*(6), 1201-12.

Zhang, R., Xue, Y.-yu, Lu, S.-duo, Wang, Yao, Zhang, L.-mei, Huang, Y.-lin, et al.
(2006). Bcl-2 enhances neurogenesis and inhibits apoptosis of newborn neurons in
adult rat brain following a transient middle cerebral artery occlusion. *Neurobiology
of Disease*, *24*, 345 - 356.

Zhang, R., Zhang, Z., Wang, L., Wang, Y., Gousev, A., Zhang, L., Ho, K.-loon, et al.
(2004). Activated Neural Stem Cells Contribute to Stroke-Induced Neurogenesis and
Neuroblast Migration Toward the Infarct Boundary in Adult Rats. *Blood*, 441-448.

Zilles, K. (1985). *The Cortex of the Rat: A Stereotaxic Atlas*. Springer-Verlag GmbH:
Berlin, Germany.